

**Final Report for 2<sup>nd</sup> Year Contract of AOARD 034032**

**Development of Advanced Oxide Dispersion Strengthened  
Tungsten Heavy Alloy for Penetrator Application**

**September 30, 2005**

Soon H. Hong  
Ho J. Ryu  
Seung I. Cha  
Hee Y. Kim  
Kyung T. Kim  
Kyong H. Lee  
Chan B. Mo

Department of Materials Science and Engineering  
Korea Advanced Institute of Science and Technology  
373-1 Kusung-dong, Yuseong-gu, Daejeon 305-701, Korea  
Tel. +82-42-869-3327, Fax. +82-42-869-3310  
e-mail [shhong@kaist.ac.kr](mailto:shhong@kaist.ac.kr)

| Report Documentation Page   |                                | Form Approved<br>OMB No. 0704-0188                      |
|---|--------------------------------|---|
| Public reporting burden for the collection of information is estimated to average 1 hour per response, including the time for reviewing instructions, searching existing data sources, gathering and maintaining the data needed, and completing and reviewing the collection of information. Send comments regarding this burden estimate or any other aspect of this collection of information, including suggestions for reducing this burden, to Washington Headquarters Services, Directorate for Information Operations and Reports, 1215 Jefferson Davis Highway, Suite 1204, Arlington VA 22202-4302. Respondents should be aware that notwithstanding any other provision of law, no person shall be subject to a penalty for failing to comply with a collection of information if it does not display a currently valid OMB control number.  |                                |   |
| 1. REPORT DATE<br><b>20 NOV 2007</b>  | 2. REPORT TYPE<br><b>Final</b> | 3. DATES COVERED<br><b>16-10-2003 to 14-11-2007</b>     |
| 4. TITLE AND SUBTITLE<br><b>Development of advanced oxide-dispersion-strengthened tungsten heavy alloy</b>  |                                | 5a. CONTRACT NUMBER<br><b>F6256203C0052</b>             |
|   |                                | 5b. GRANT NUMBER  |
|   |                                | 5c. PROGRAM ELEMENT NUMBER                              |
| 6. AUTHOR(S)<br><b>Soon-Hyung Hong</b>  |                                | 5d. PROJECT NUMBER                                      |
|   |                                | 5e. TASK NUMBER   |
|   |                                | 5f. WORK UNIT NUMBER                                    |
| 7. PERFORMING ORGANIZATION NAME(S) AND ADDRESS(ES)<br><b>Korea Advanced Institute of Science &amp; Technology, 373-1 Kusung-dong, Yusung-gu, Daejeon 305-701, Korea (South), KS, N/A</b>  |                                | 8. PERFORMING ORGANIZATION REPORT NUMBER<br><b>N/A</b>  |
| 9. SPONSORING/MONITORING AGENCY NAME(S) AND ADDRESS(ES)<br><b>AOARD, UNIT 45002, APO, AP, 96337-5002</b>  |                                | 10. SPONSOR/MONITOR'S ACRONYM(S)<br><b>AOARD-034032</b> |
|   |                                | 11. SPONSOR/MONITOR'S REPORT NUMBER(S)                  |
| 12. DISTRIBUTION/AVAILABILITY STATEMENT<br><b>Approved for public release; distribution unlimited</b>   |                                |   |
| 13. SUPPLEMENTARY NOTES   |                                |   |
| 14. ABSTRACT<br><p><b>The effects of fabrication process parameters, including conditions for powder preparation, sintering, cyclic heat-treatment, swaging, and annealing processes, on microstructures and static/dynamic mechanical properties of ODS tungsten heavy alloys were investigated. The composition of ODS tungsten heavy alloys was designed as 94W-4.56Ni-1.14Co-0.3Y2O3 which show the highest strength at similar microstructural parameters based on the analysis of microstructures and mechanical properties. The two-stage sintered ODS tungsten heavy alloy showed finer tungsten grain size than those prepared by conventional liquid phase sintering with similar matrix volume fraction and tungsten/tungsten contiguity. Cyclic heat-treatment process was introduced after sintering process to increase the tensile strength and elongation by decreasing the tungsten/tungsten contiguity. The swaging and annealing processes of ODS tungsten heavy alloy increase the tensile strength with decreasing the elongation. High strain rate dynamic compressive tests were performed by Hopkinson pressure bar test equipment. The dynamic compressive strength of ODS tungsten heavy alloys was improved by addition of oxide dispersoids and by modification of composition from W-Ni-Fe to W-Ni-Co. At the same time, the adiabatic shear bands induced by high strain rate dynamic shear tests became narrower by the dispersion of Y2O3 and by the composition modification. The 94W-4.56Ni-1.14Co-0.3Y2O3 alloy, which was two-stage sintered, cyclic heat-treated, swaged, and annealed, shows high ultimate tensile strength of 1350MPa, moderate elongation of 5% and high compressive yield strength of 1800MPa under a high strain rate deformation of 3000/s. The 94W-4.56Ni-1.14Co-0.3Y2O3 ODS tungsten heavy alloy has been suggested as an advanced core material for kinetic energy penetrators and hard target penetrators.</b></p> |                                |   |
| 15. SUBJECT TERMS   |                                |   |

|                                  |                                    |                                     |  |                                     |                                    |
|----------------------------------|------------------------------------|-------------------------------------|--|-------------------------------------|------------------------------------|
| 16. SECURITY CLASSIFICATION OF:  |                                    |                                     | 17. LIMITATION OF<br>ABSTRACT<br><b>Same as<br/>Report (SAR)</b> | 18. NUMBER<br>OF PAGES<br><b>54</b> | 19a. NAME OF<br>RESPONSIBLE PERSON |
| a. REPORT<br><b>unclassified</b> | b. ABSTRACT<br><b>unclassified</b> | c. THIS PAGE<br><b>unclassified</b> |  |                                     |                                    |

## Abstract

The composition of oxide dispersion strengthened (ODS) tungsten heavy alloys was modified from the W-Ni-Fe-Y<sub>2</sub>O<sub>3</sub> alloy to W-Ni-Fe-Mo-Y<sub>2</sub>O<sub>3</sub> and W-Ni-Co-Y<sub>2</sub>O<sub>3</sub> alloys. Elemental powders of tungsten, nickel, iron, molybdenum, cobalt and yttria corresponding to designed compositions, which are 94W-4.56Ni-1.14Fe-0.3Y<sub>2</sub>O<sub>3</sub>, 94W-3.65Ni-0.91Fe-1.14Mo-0.3Y<sub>2</sub>O<sub>3</sub> and 94W-4.56Ni-1.14Co-0.3Y<sub>2</sub>O<sub>3</sub>, were mechanically alloyed in a planetary mill for 6 hrs. 94W-4.56Ni-1.14Co-0.3Y<sub>2</sub>O<sub>3</sub> alloy showed higher strength at room and elevated temperature, but showed lower elongation and impact energy than 94W-4.56Ni-1.14Fe-0.3Y<sub>2</sub>O<sub>3</sub> and 94W-3.65Ni-0.91Fe-1.14Mo-0.3Y<sub>2</sub>O<sub>3</sub> alloys. The effects of two-stage sintering process and cyclic heat-treatment process on microstructure and mechanical properties of ODS tungsten heavy alloys were investigated. Mechanically alloyed powders were solid state sintered at 1300-1450°C for 1hr in hydrogen atmosphere, and followed by liquid phase sintering at 1465-1505°C up to 60min. The microstructure of ODS tungsten heavy alloys showed contiguous tungsten grains after solid state sintering as first stage sintering process. The microstructure of solid state sintered ODS tungsten heavy alloy was changed into spherical tungsten grains embedded in Ni-Fe-W matrix during liquid phase sintering as second stage sintering process. The two-stage sintered ODS tungsten heavy alloys from mechanically alloyed powders showed finer tungsten grain size than those of conventional liquid phase sintered tungsten heavy alloys with similar matrix volume fraction and tungsten/tungsten contiguity. Cyclic heat-treatment process was introduced after sintering to increase the elongation and impact energy by decreasing the tungsten/tungsten contiguity. The mechanical properties of ODS tungsten heavy alloys are dependent on the microstructural parameters, such as tungsten grain size, matrix volume fraction and tungsten/tungsten contiguity, which can be controlled through the two-stage sintering and the cyclic heat-treatment processes.

## Contents

|   |           |
|---|-----------|
| <b>1. Introduction</b>  | <b>4</b>  |
| <b>2. Experimental Procedures</b>   | <b>5</b>  |
| 2-1. Design and mechanical alloying of ODS tungsten heavy alloys  | 5         |
| 2-2. Sintering and heat-treatment processes of ODS tungsten heavy alloys  | 5         |
| 2-3. Characterization of mechanical properties of ODS tungsten heavy alloys   | 6         |
| <b>3. Results and Discussion</b>  | <b>9</b>  |
| 3-1. Effect of matrix modification on microstructure and mechanical properties of ODS tungsten heavy alloys           | 9         |
| 3-2. Effect of sintering process on microstructure and mechanical properties of ODS tungsten heavy alloys             | 18        |
| 3-3. Effect of cyclic heat-treatment process on microstructure and mechanical properties of ODS tungsten heavy alloys | 34        |
| 3-4. Relationship between microstructure and mechanical properties of ODS tungsten heavy alloys                       | 39        |
| <b>4. Summary</b>   | <b>43</b> |
| <b>5. References</b>  | <b>45</b> |

## 1. Introduction

Oxide dispersion strengthened (ODS) tungsten heavy alloys have been investigated as high density structural materials for kinetic energy penetrators [1, 2]. The understanding of fundamental strengthening and fracture mechanisms of tungsten heavy alloys is very important to improve the penetration performance of tungsten heavy alloys. Our previous researches [2] on ODS tungsten heavy alloy showed that the high temperature strength of tungsten heavy alloy can be enhanced by addition of ultra-fine oxide dispersoids in tungsten heavy alloy. Furthermore, the fracture mechanism of tungsten heavy alloy can be controlled in a broad range from brittle fracture mode to ductile fracture mode by addition of oxide dispersoids. These results strongly support that the self-sharpening behavior of tungsten heavy alloy could be enhanced by the homogeneous distribution of ultra-fine oxide particles. Even though the previous research results have verified the possibilities to improve the penetration performance of tungsten heavy alloy by addition of ultra-fine oxide particles as a strengthening agent, the optimization of sintering process and microstructure needs to be investigated further.

In this study, as second year contract for AOARD 034032, composition modification, two-stage sintering process and cyclic heat-treatment process of mechanically alloyed ODS tungsten heavy alloys were suggested in order to control the microstructure and mechanical properties. For composition modification, W-Ni-Co-Y<sub>2</sub>O<sub>3</sub> alloy was introduced for enhanced mechanical properties. In two-stage sintering process, solid state sintering was carried out to achieve full densification of mechanically alloyed ODS tungsten heavy alloy as a first stage sintering process. The liquid phase sintering with rapid heating rate and short holding time is followed to control the microstructural parameters such as tungsten grain size, tungsten/tungsten contiguity and matrix volume fraction as second stage sintering. Cyclic heat-treatment process was performed to control the tungsten/tungsten contiguity and the mechanical properties of ODS tungsten heavy alloys. In addition, the relationship between microstructure and mechanical properties of ODS tungsten heavy alloys controlled by composition modification, two-stage sintering process and heat-treatment process was investigated.

## **2. Experimental Procedures**

### **2-1. Design and mechanical alloying of ODS tungsten heavy alloys**

The fabrication process and composition of ODS tungsten heavy alloy were designed based on first year research on ODS tungsten heavy alloy [2]. The elemental powders of W, Ni, Fe, Mo, Co and  $Y_2O_3$  were weighed based on the designed compositions. The composition of ODS tungsten heavy alloys was modified from the conventional 94W-4.56Ni-1.14Fe-0.3 $Y_2O_3$  alloy to new designed 94W-3.65Ni-0.91Fe-1.14Mo-0.3 $Y_2O_3$  and 94W-4.56Ni-1.14Co-0.3 $Y_2O_3$  alloys.

The powders were mechanically alloyed using a planetary mill supplied by Fritsch GmbH. Two mechanical alloying processes are suggested; one is mechanical alloying and mixing process, and the other is two-step mechanical alloying process. In mechanical alloying and mixing process, tungsten and yttria powders were mechanically alloyed firstly, and then mechanically alloyed powder and metal matrix powders were blended by conventional ball milling. In two-step mechanical alloying process, tungsten and yttria powders were mechanically alloyed firstly, and the powders were mechanically alloyed again with metal matrix powders such as nickel, iron, molybdenum and cobalt into designed compositions.

The ball-to-powder ratio was 10:1 with a fixed ball-filling ratio of 0.3 and total ball weight of 500g. The mechanical alloying speed and time were 200 rpm and 6 hours, respectively.

### **2-2. Sintering and heat-treatment processes of ODS tungsten heavy alloys**

The mechanically alloyed powders were consolidated into green compacts by die compaction under a pressure of 200MPa. The green compacts were solid state sintered at various temperatures from 1300 to 1450°C for 1 hr in hydrogen atmosphere. Solid state sintered ODS tungsten heavy alloy was subsequently liquid phase sintered at the temperature ranged from 1465 to 1505°C for 0 ~ 60min in argon atmosphere by rapidly pushing the specimens into the hot zone of furnace. Fig. 1 shows a two-stage sintering temperature cycle when the secondary sintering temperature is 1485°C and the secondary sintering time is 0min.

The sintered specimens were subjected to cyclic heat-treatment which consisted of repeated isothermal holdings at 1150°C for 5min in nitrogen atmosphere. Water

quenching was performed after each isothermal holding to prevent hydrogen embrittlement and impurity segregation during the cooling.

The density of sintered ODS tungsten heavy alloys was measured according to ASTM D792 standard. The average tungsten grain size, volume fraction of matrix phase and tungsten/tungsten contiguity of sintered ODS tungsten heavy alloys were characterized by optical and scanning electron microscopy.

### **2-3. Characterization of mechanical properties of ODS tungsten heavy alloys**

The static mechanical properties of ODS tungsten heavy alloys were characterized by tensile tests based on ASTM E-8M. The specimens were prepared by compacting into near-net shape and followed by sintering and heat treatment as described above. The tensile tests were performed under constant strain rate of  $6.67 \times 10^{-4}$ /s using Instron 5583 machine. The strain of specimens was measured by an extensometer. The yield strength, ultimate tensile strength and elongation of ODS tungsten heavy alloys were characterized and analyzed from the tensile test data.

High temperature compressive tests were performed using the hot working simulator named as Thermecmaster-Z. The cylindrical specimens with 5mm in diameter and 7.5mm in height were used for high temperature compressive tests. The compression temperature was 800°C under an initial strain rate of  $10^1$ /s. The high temperature compressive tests were performed in Ar atmosphere to avoid oxidation of specimens during the test.

The impact properties of ODS tungsten heavy alloys were characterized by Charpy impact tests, which were performed on notched samples in ASTM E-24 as shown in Fig.2.



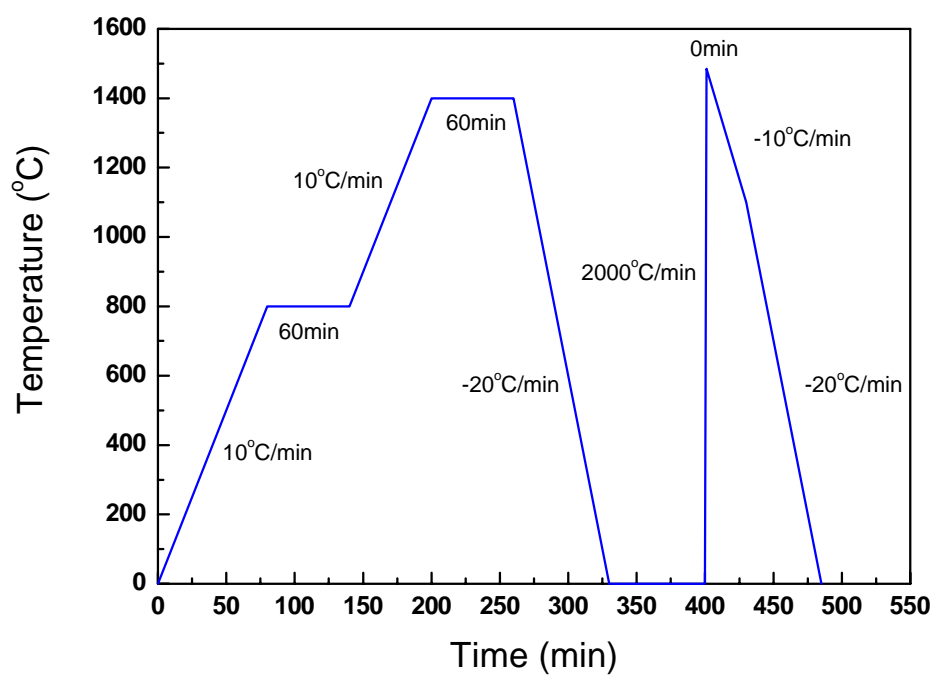


Fig. 1. The sintering temperature profile for a two-stage sintering of ODS tungsten heavy alloys, when the secondary sintering is carried out at 1485 °C for 0 min.

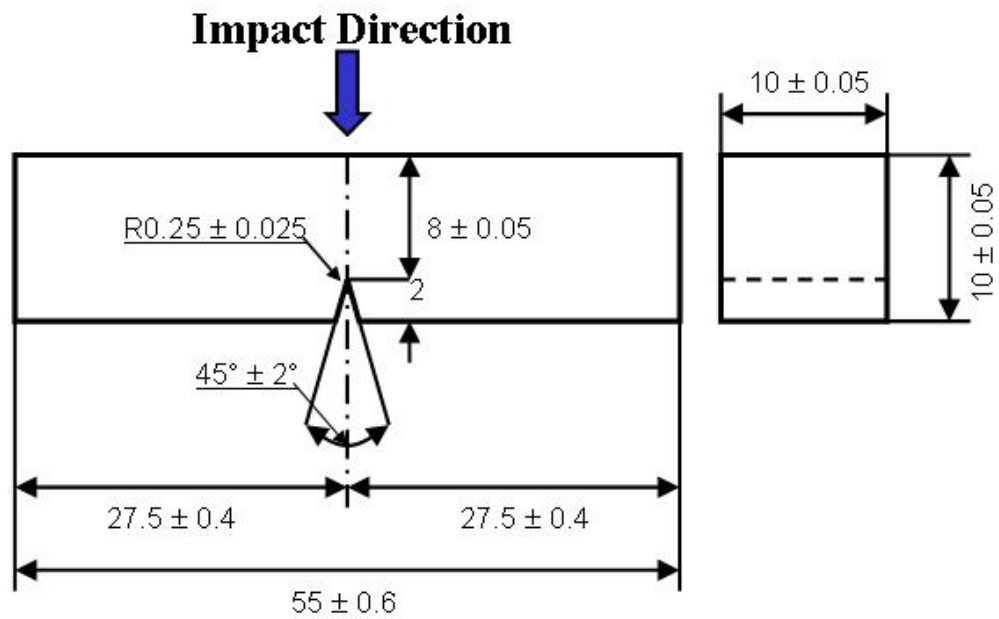


Fig. 2. The design of specimens with thickness of 10mm, width of 10mm and length of 55mm, and V-notched with 2mm depth and  $45^\circ$  angle for impact test.

### 3. Results and Discussion

#### 3-1. Effect of matrix modification on microstructure and mechanical properties of ODS tungsten heavy alloys

New compositions of ODS tungsten heavy alloys, 94W-4.56Ni-1.14Fe-0.3Y<sub>2</sub>O<sub>3</sub> and 94W-3.65Ni-0.91Fe-1.14Mo-0.3Y<sub>2</sub>O<sub>3</sub>, were designed for modification of the matrix composition of ODS tungsten heavy alloy. The Ni-Fe-Mo pre-alloyed powder for matrix was prepared by mechanical alloying of nickel, iron and molybdenum powders. The composition of the pre-alloyed powder designed by theoretical calculations was 3.65Ni-0.91Fe-1.14Mo. In previous studies [3,4], alloying of Mo decreases the solubility of tungsten in matrix and it can restrain the growth of tungsten grains during the sintering. Fig. 3(a) and (b) show the microstructures of 94W-4.56Ni-1.14Fe-0.3Y<sub>2</sub>O<sub>3</sub> and 94W-3.65Ni-0.91Fe-1.14Mo-0.3Y<sub>2</sub>O<sub>3</sub> alloys. The microstructure of 94W-3.65Ni-0.91Fe-1.14Mo-0.3Y<sub>2</sub>O<sub>3</sub> alloy shows similar morphology to that of 94W-4.56Ni-1.14Fe-0.3Y<sub>2</sub>O<sub>3</sub> alloy after sintering at the temperature of 1485°C.

New composition of 94W-4.56Ni-1.14Co-0.3Y<sub>2</sub>O<sub>3</sub> alloy was also designed by substituting Fe with Co. 94W-4.56Ni-1.14Co-0.3Y<sub>2</sub>O<sub>3</sub> alloy was fabricated with Ni:Co ratio of 4:1 in order to compare with 94W-4.56Ni-1.14Fe-0.3Y<sub>2</sub>O<sub>3</sub> alloy. Unlike the Ni-Fe system, Ni and Co are completely soluble to each other. The W-Ni-Co-Y<sub>2</sub>O<sub>3</sub> alloy has higher eutectic temperature, by about 20°C, than that of W-Ni-Fe-Y<sub>2</sub>O<sub>3</sub> alloy when the Ni:Fe or Ni:Co ratio is 4:1, as shown in Fig. 4. Fig. 3(c) and (d) show the microstructures of 94W-4.56Ni-1.14Co-0.3Y<sub>2</sub>O<sub>3</sub> alloys. At a same sintering temperature of 1485°C, W-Ni-Co-Y<sub>2</sub>O<sub>3</sub> alloys showed finer tungsten grain size compared to those of W-Ni-Fe-Y<sub>2</sub>O<sub>3</sub> alloys. The microstructure of 94W-4.56Ni-1.14Co-0.3Y<sub>2</sub>O<sub>3</sub> alloy sintered at 1505°C showed similar morphology to that of 94W-4.56Ni-1.14Fe-0.3Y<sub>2</sub>O<sub>3</sub> alloy sintered at 1485°C.

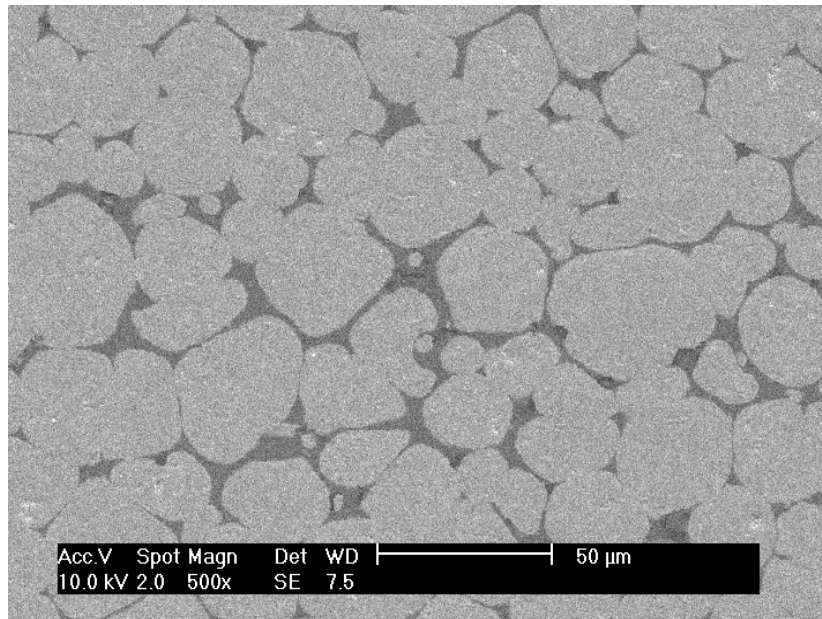
The quantitative analysis of microstructural parameters such as tungsten grain size, matrix volume fraction and tungsten/tungsten contiguity according to the composition and sintering temperature was performed as shown in Fig. 5. The variation of microstructural parameters showed same tendency according to the sintering temperature regardless of matrix composition.

Fig. 6 shows the effect of matrix compositions on tensile properties of ODS tungsten heavy alloys. The yield strength and ultimate tensile strength of 94W-3.65Ni-0.91Fe-1.14Mo-0.3Y<sub>2</sub>O<sub>3</sub> alloy were similar to those of 94W-4.56Ni-1.14Fe-

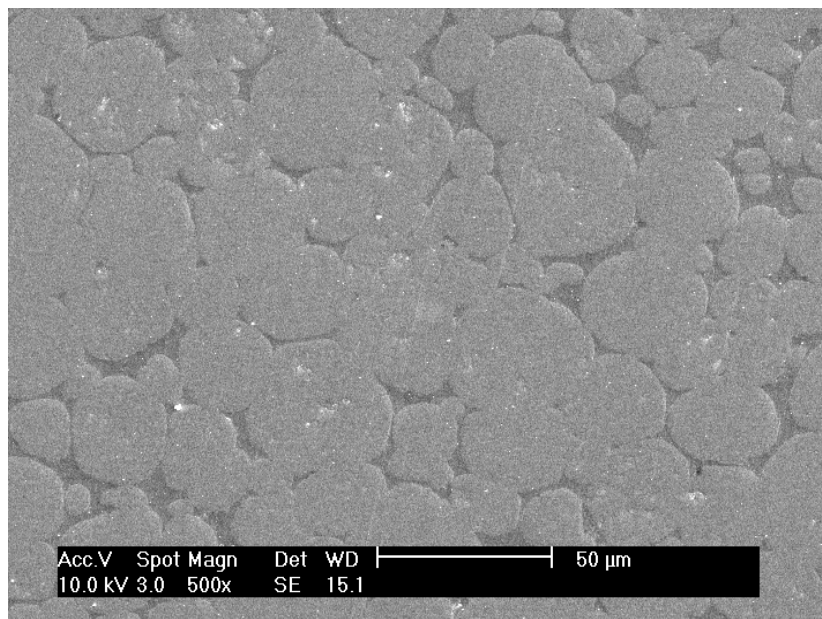
0.3Y<sub>2</sub>O<sub>3</sub> alloy at a same sintering condition. Also, 94W-3.65Ni-0.91Fe-1.14Mo-0.3Y<sub>2</sub>O<sub>3</sub> alloy showed lower elongation due to lower volume fraction of matrix. 94W-4.56Ni-1.14Co-0.3Y<sub>2</sub>O<sub>3</sub> alloy showed the highest yield strength and ultimate tensile strength among three alloys. However, the lowest elongation can be seen in 94W-4.56Ni-1.14Co-0.3Y<sub>2</sub>O<sub>3</sub> alloy.

High temperature yield strength of 94W-4.56Ni-1.14Co-0.3Y<sub>2</sub>O<sub>3</sub> alloy was higher than those of 94W-4.56Ni-1.14Fe-0.3Y<sub>2</sub>O<sub>3</sub> and 94W-3.65Ni-0.91Fe-1.14Mo-0.3Y<sub>2</sub>O<sub>3</sub> alloys as shown in Fig. 7. However, 94W-4.56Ni-1.14Co-0.3Y<sub>2</sub>O<sub>3</sub> alloy showed the lowest impact energy.

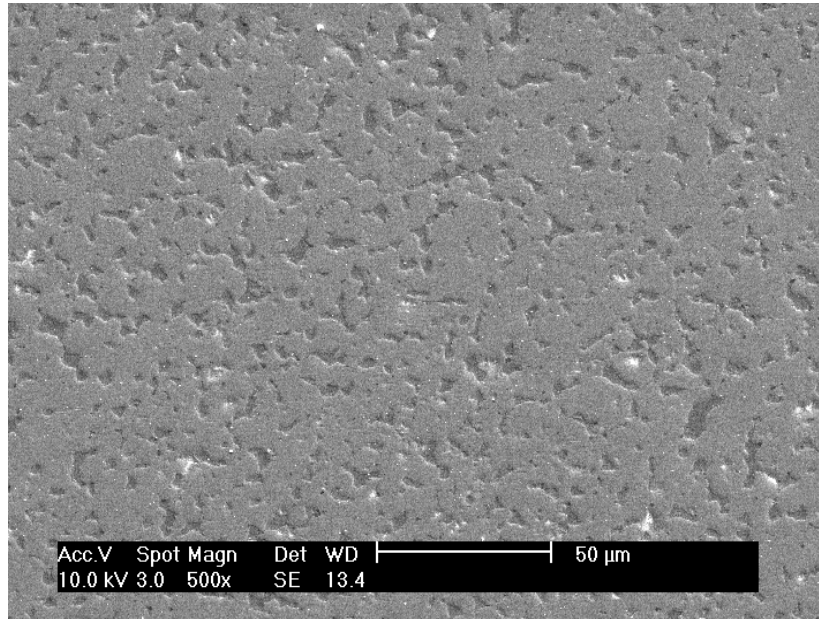
Based on the controlled microstructure and mechanical properties of ODS tungsten heavy alloys, 94W-4.56Ni-1.14Co-0.3Y<sub>2</sub>O<sub>3</sub> alloy showed improved strength at room and elevated temperature compared to those of 94W-4.56Ni-1.14Fe-0.3Y<sub>2</sub>O<sub>3</sub> and 94W-3.65Ni-0.91Fe-1.14Mo-0.3Y<sub>2</sub>O<sub>3</sub> alloys.



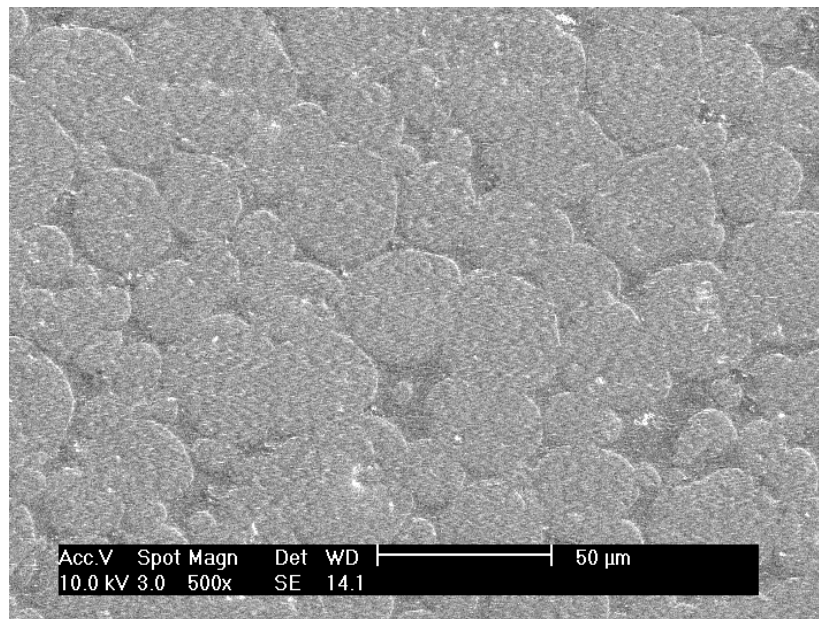
(a)



(b)

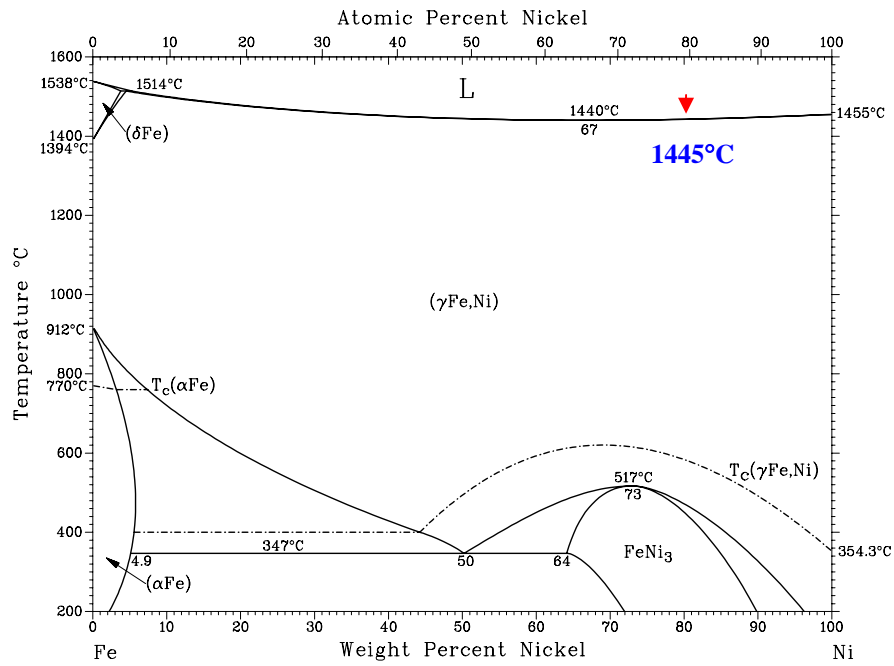


(c)

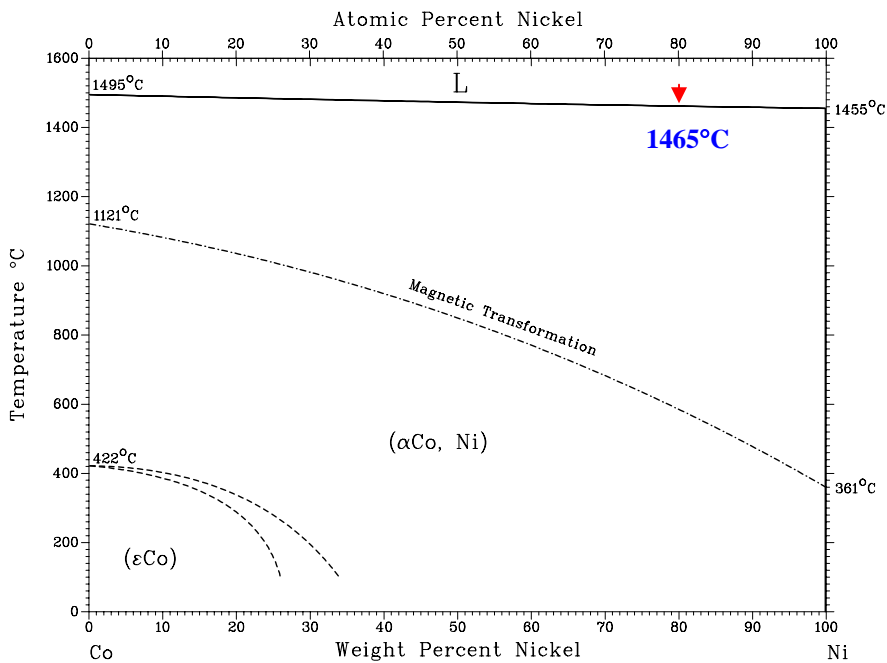


(d)

Fig. 3. Microstructure of ODS tungsten heavy alloys with various compositions. (a) 94W-4.56Ni-1.14Fe-0.3Y<sub>2</sub>O<sub>3</sub>, (b) 94W-3.65Ni-0.91Fe-1.14Mo-0.3Y<sub>2</sub>O<sub>3</sub> and (c) 94W-4.56Ni-1.14Co-0.3Y<sub>2</sub>O<sub>3</sub> sintered at 1485°C for 1 hour, and (d) 94W-4.56Ni-1.14Co-0.3Y<sub>2</sub>O<sub>3</sub> sintered at 1505°C for 1 hour.

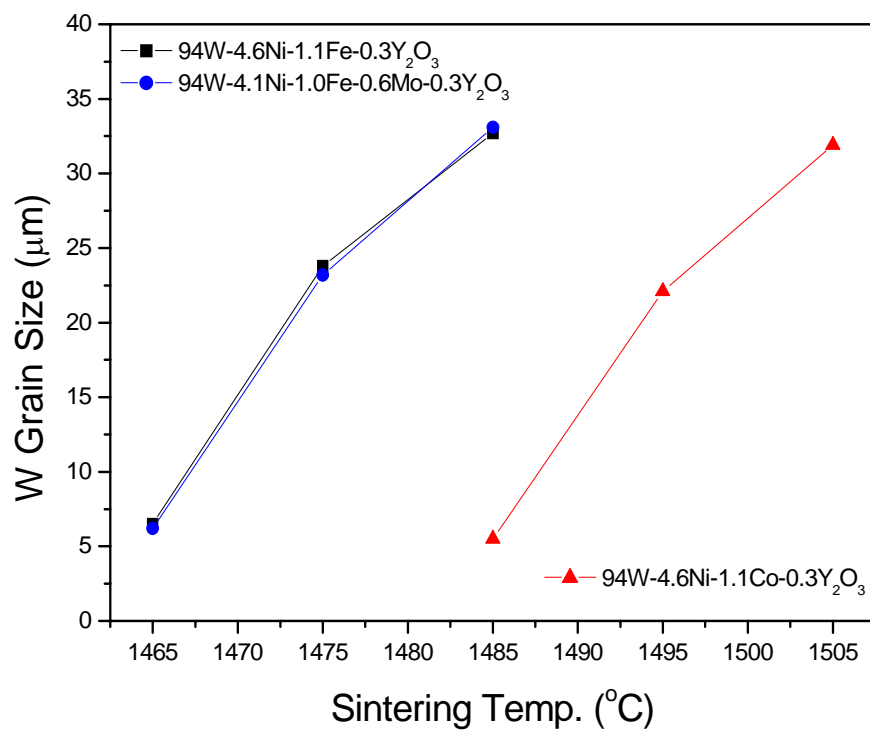


(a)

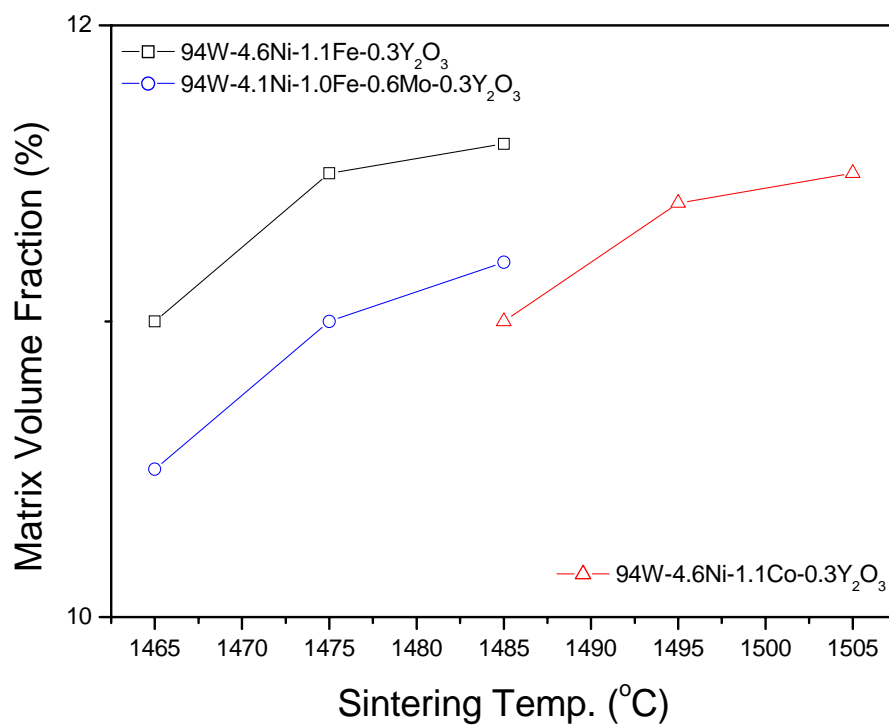


(b)

Fig. 4. The phase diagrams for (a) Ni-Fe system and (b) Ni-Co system (ASM handbook).



(a)



(b)



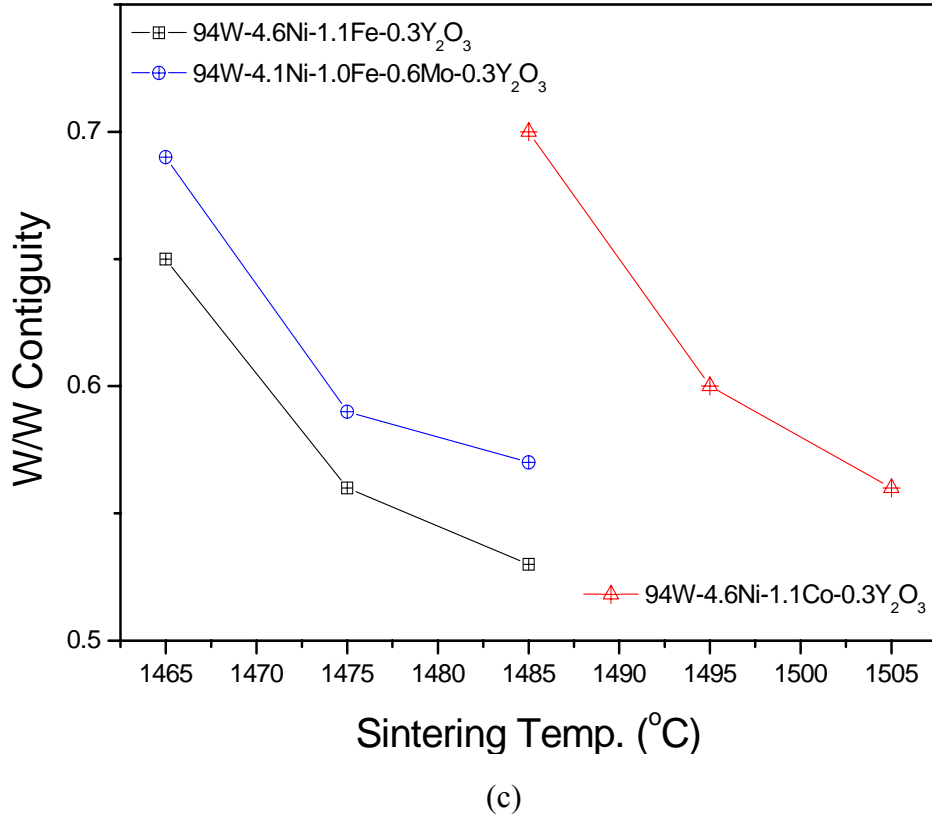


Fig. 5. The variation of microstructure parameters of sintered ODS tungsten heavy alloys according to the sintering temperature, (a) W grain size, (b) matrix volume fraction and (c) W/W contiguity. The tungsten heavy alloys were sintered for 1 hour.

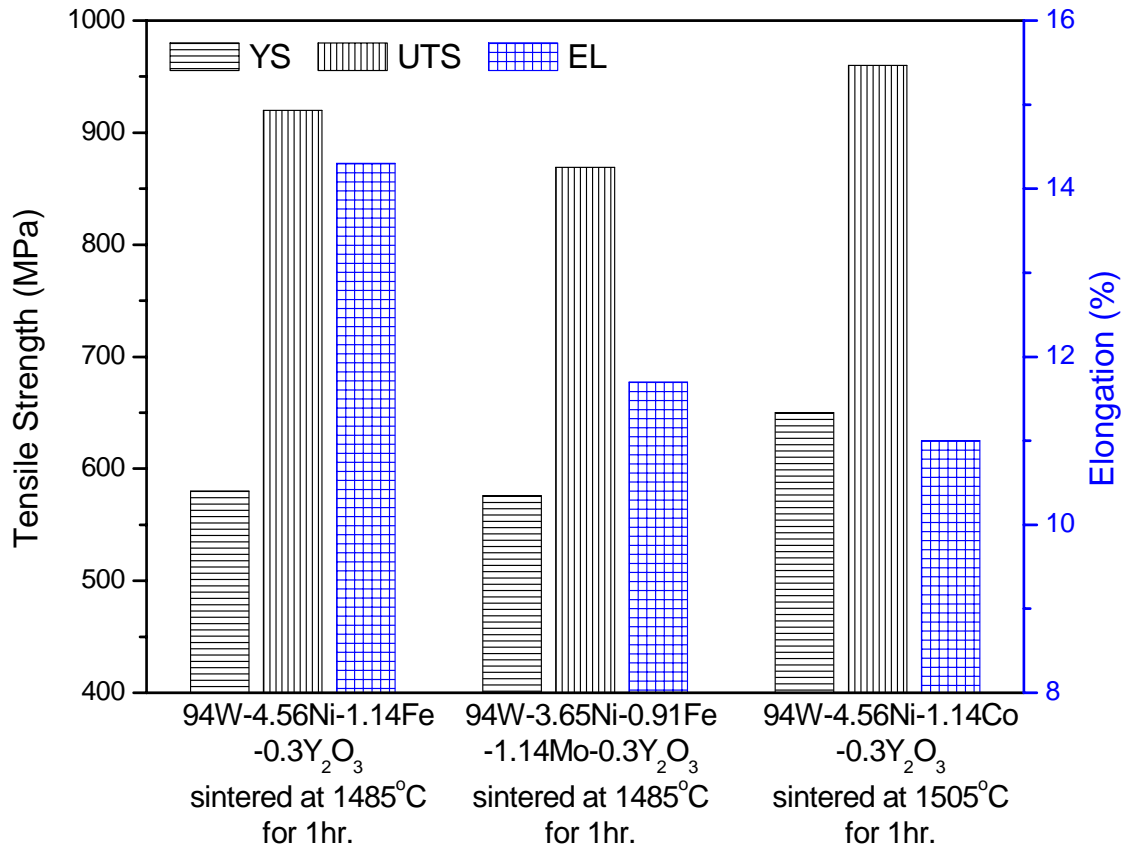


Fig. 6. Tensile properties of ODS tungsten heavy alloys according to the composition.

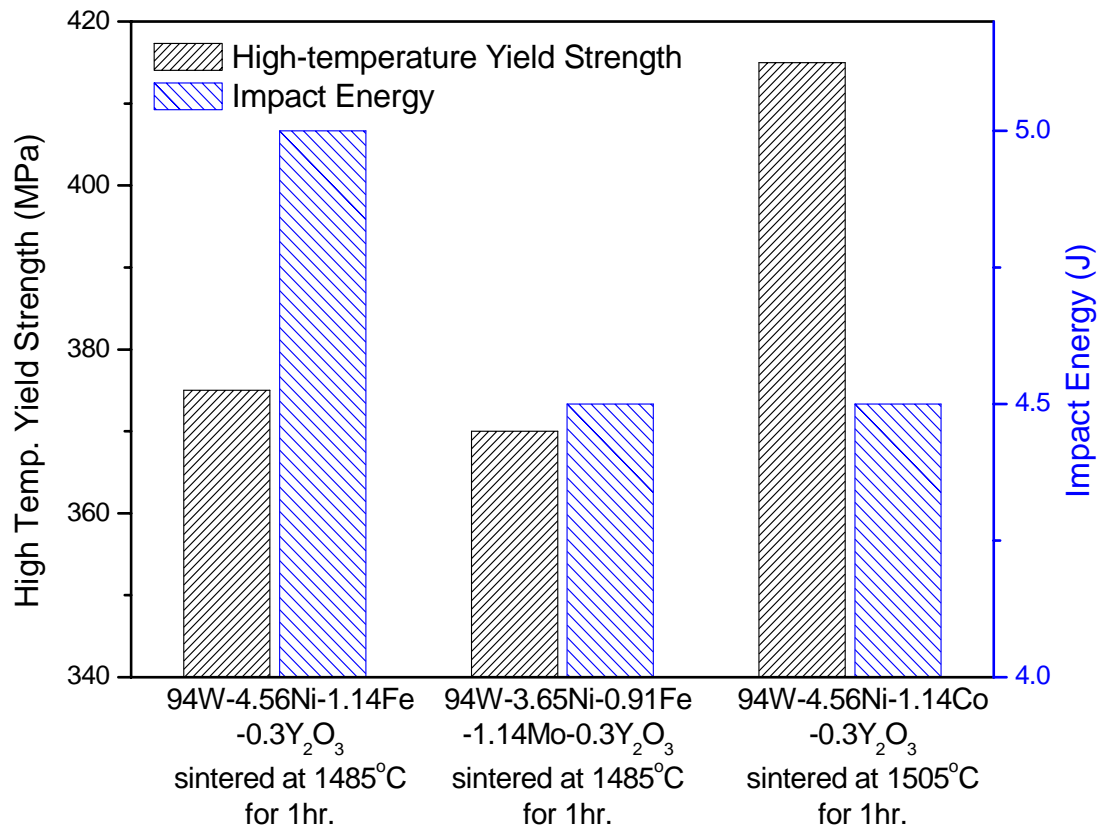


Fig. 7. High-temperature strength and impact energy of ODS tungsten heavy alloys according to the composition.

### **3-2. Effect of sintering process on microstructure and mechanical properties of ODS tungsten heavy alloys**

The effect of location of oxide dispersoids in tungsten heavy alloy was investigated in first year research by the modification of mechanical alloying process [2]. Fig. 8 shows the microstructure of solid state sintered 94W-4.56Ni-1.14Fe-0.3Y<sub>2</sub>O<sub>3</sub> alloy at the temperature ranged from 1300 to 1450 °C for 1hr from the powders prepared by mechanical alloying and mixing process. Matrix phase was not homogeneously distributed and formed matrix pool as shown in Fig. 8. Solid state sintered ODS tungsten heavy alloys showed relative density ranged from 90 to 97 %. The relative density of ODS tungsten heavy alloy increased above 99 % after secondary sintering at 1465 °C for 1 min as shown in Fig. 10. However, as shown in Fig. 9, the matrix pool was not removed by the secondary sintering process.

Fig. 11 shows the microstructure of the solid state sintered 94W-4.56Ni-1.14Fe-0.3Y<sub>2</sub>O<sub>3</sub> alloy at the temperature ranged from 1300 to 1450 °C for 1hr from the powder prepared by two-step mechanical alloying process. When the ODS tungsten heavy alloy powders were fabricated by two-step mechanical alloying process, the matrix phase was homogeneously distributed as shown in Fig. 11. When the 94W-4.56Ni-1.14Fe-0.3Y<sub>2</sub>O<sub>3</sub> alloy was solid state sintered at 1400-1450 °C for 1 hr, the tungsten grains were interconnected each other. The average tungsten grain size in the solid state sintered alloys was below 3 μm. These results indicate that the mechanical alloying followed by solid-state sintering is very effective for refining the microstructure of ODS tungsten heavy alloys. Considering the homogeneous microstructure and relative density, solid state sintering temperature of 1400 °C and sintering time of 1hr after two-step mechanical alloying process could be applicable to the two-stage sintering process.

The matrix volume fraction and tungsten/tungsten contiguity of ODS tungsten heavy alloys, solid state sintered at 1400 °C for 1 hr, were measured as 7.3 % and 0.75, respectively. Comparing to the conventional ODS tungsten heavy alloys liquid phase sintered with the same composition [2], matrix volume fraction decreased and tungsten/tungsten contiguity increased by solid state sintering of ODS tungsten heavy alloys. The volume fraction of matrix phase decreased due to the decrease of the tungsten solubility in the matrix at lower sintering temperature. The increase in tungsten/tungsten contiguity is due to the decrease of matrix volume fraction and the increase of dihedral angle between tungsten grains in the matrix phase at lower sintering temperature [5].

Fig. 12 shows the microstructure of two-stage sintered 94W-4.56Ni-1.14Fe-0.3Y<sub>2</sub>O<sub>3</sub> alloys, which were first stage sintered at 1400 °C for 1 hr, and followed by second stage sintered at temperature ranged from 1465 to 1485 °C for 30 min. Tungsten grains in ODS tungsten heavy alloy, secondary liquid phase sintered at 1465 °C for 30min, remained as highly contiguous shape similar to those solid state sintered at 1300-1450 °C for 1 hr. However, the shape of tungsten grains becomes spherical after secondary sintering above 1475 °C. The tungsten grain size and matrix volume fraction increased, but tungsten/tungsten contiguity decreased with increasing the secondary sintering temperature as shown in Fig. 13.

The effect of secondary sintering time at a temperature of 1485°C on microstructure of 94W-4.56Ni-1.14Fe-0.3Y<sub>2</sub>O<sub>3</sub> alloy was investigated. The average tungsten grain size increased from 1.8 to 19.8 μm with increasing the secondary sintering time from 0 to 60 min as shown in Fig. 14. The relationship between tungsten grain size and secondary sintering time was found to satisfy the LSW theory [6, 7] with diffusion control process as followed:

$$\bar{r}_t^3 - \bar{r}_o^3 = k(t - t_o) \quad (1)$$

where  $\bar{r}_t$  is average radius of particles at time,  $t$ ,  $\bar{r}_o$  is average radius of particles at time,  $t_o$ , and  $k$  is a coarsening rate constant. The coarsening rate constant,  $k$ , for a mechanically alloyed 94W-4.56Ni-1.14Fe-0.3Y<sub>2</sub>O<sub>3</sub> alloy was measured as 16.5 μm<sup>3</sup> min<sup>-1</sup> at 1485 °C as shown in Fig. 15. The tungsten grain size of a two-stage sintered ODS tungsten heavy alloys can be controlled by the secondary sintering time in the two-stage sintering process. Two-stage sintered 94W-4.56Ni-1.14Fe-0.3Y<sub>2</sub>O<sub>3</sub> alloy showed finer tungsten grain size of 19.3 μm with similar matrix volume fraction and tungsten/tungsten contiguity compared to the conventional liquid phase sintered ODS tungsten heavy alloy [2].

The effect of secondary sintering temperature on yield and tensile strength of two-stage sintered 94W-4.56Ni-1.14Fe-0.3Y<sub>2</sub>O<sub>3</sub> alloy was shown in Fig. 16(a). The yield strength of ODS tungsten heavy alloys was sensitive to secondary sintering temperature from 1465 to 1485°C. With increasing the secondary sintering temperature, the yield strength decreased from 893 to 661MPa, but ultimate tensile strength remained similar level of about 950MPa. The elongation of ODS tungsten heavy alloy increased with increasing the sintering temperature as shown in Fig. 16(b). The elongation of two-stage sintered ODS tungsten heavy alloys increased from 0.5 to 11% with increasing the secondary sintering temperature.

The effect of secondary sintering time on yield strength and ultimate tensile strength of two-stage sintered 94W-4.56Ni-1.14Fe-0.3Y<sub>2</sub>O<sub>3</sub> alloy was shown in Fig. 17(a). The yield strength of ODS tungsten heavy alloys decreased from 952 to 639MPa, at the same time, the ultimate tensile strength decreased from 1000 to 883MPa with increasing the secondary sintering time from 5 to 60min. The elongation of two-stage sintered ODS tungsten heavy alloys increases with increasing the secondary sintering time as shown in Fig. 17(b). In the case of ODS tungsten heavy alloys secondarily sintered at 1485°C for 0-3min, they showed brittle fracture without macroscopic yielding behavior. However, the elongation of ODS tungsten heavy alloy increased to 12.3% when sintered for 60min.

At the same time, effect of two-stage sintering process on microstructure and mechanical properties of 94W-4.56Ni-1.14Co-0.3Y<sub>2</sub>O<sub>3</sub> alloys was investigated. The yield strength and ultimate tensile strength decreased, but the elongation increased with increasing the secondary sintering temperature as shown in Fig. 18. The yield strength and ultimate tensile strength decreased with increasing the secondary sintering time as shown in Fig. 19. The variation for mechanical properties of two-stage sintered 94W-4.56Ni-1.14Co-0.3Y<sub>2</sub>O<sub>3</sub> alloys with increasing the secondary sintering temperature and time showed same trend compared with those of 94W-4.56Ni-1.14Fe-0.3Y<sub>2</sub>O<sub>3</sub> alloys.

Fig. 20 shows the effect of compositions on tensile properties of two-stage sintered ODS tungsten heavy alloys. 94W-4.56Ni-1.14Co-0.3Y<sub>2</sub>O<sub>3</sub> alloy showed higher yield strength and ultimate tensile strength, and lower elongation compared with that of 94W-4.56Ni-1.14Fe-0.3Y<sub>2</sub>O<sub>3</sub> alloy.

In summary, two-stage sintered ODS tungsten heavy alloy showed finer tungsten grain size and higher tensile strength compared to the conventional liquid phase sintered ODS tungsten heavy alloy. Microstructure and mechanical properties of a two-stage sintered ODS tungsten heavy alloys can be controlled by controlling the secondary sintering conditions.

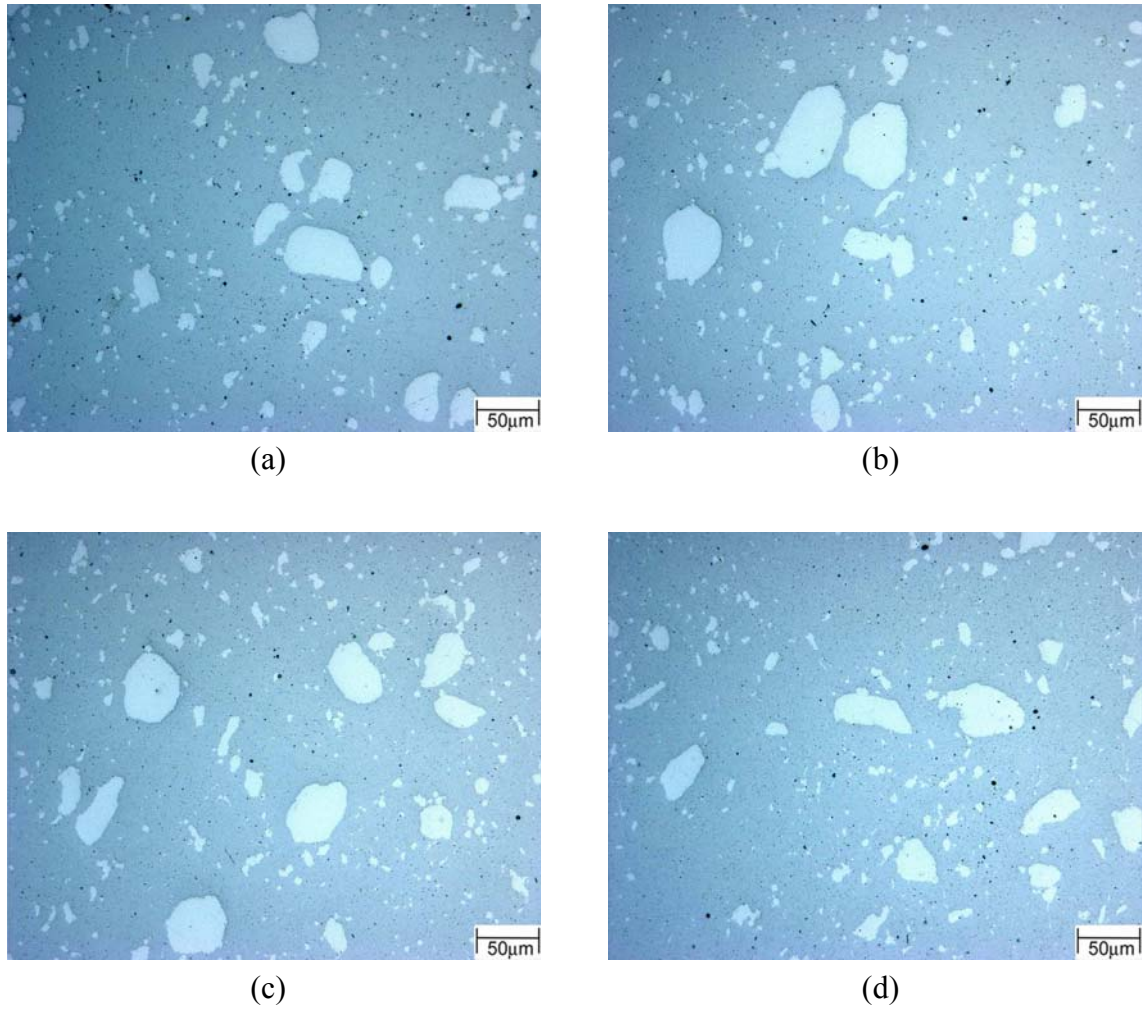


Fig. 8. Microstructure of the solid state sintered  $94\text{W}-4.56\text{Ni}-1.14\text{Fe}-0.3\text{Y}_2\text{O}_3$  tungsten heavy alloy at (a)  $1300^\circ\text{C}$ , (b)  $1350^\circ\text{C}$ , (c)  $1400^\circ\text{C}$  and (d)  $1450^\circ\text{C}$  for 1 hr from the powders prepared by mechanical alloying and mixing process.

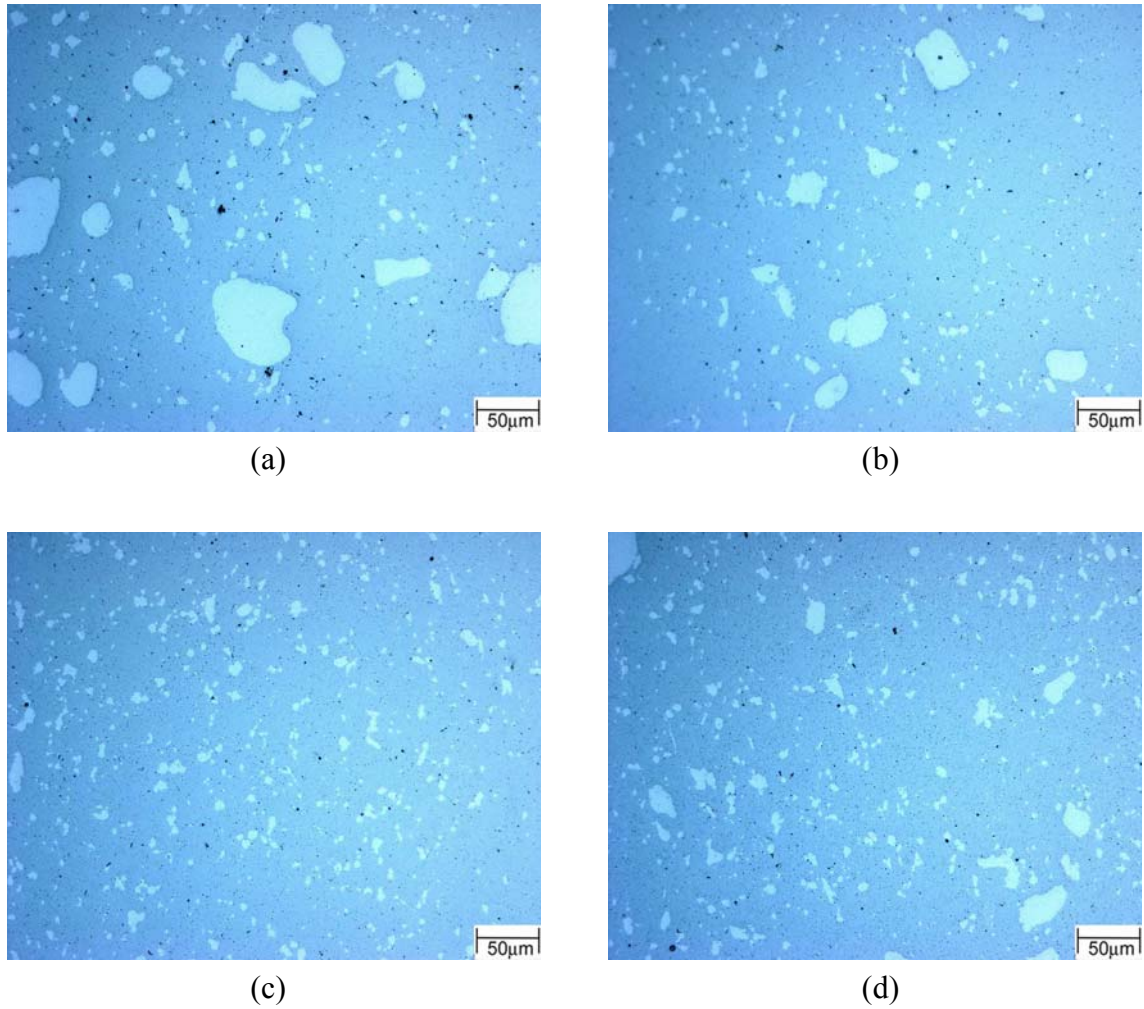


Fig. 9. Microstructure of the secondarily sintered  $94\text{W}-4.56\text{Ni}-1.14\text{Fe}-0.3\text{Y}_2\text{O}_3$  tungsten heavy alloys at  $1465^\circ\text{C}$  for 1 min after solid state sintering at (a)  $1300^\circ\text{C}$ , (b)  $1350^\circ\text{C}$ , (c)  $1400^\circ\text{C}$  and (d)  $1450^\circ\text{C}$  for 1 hr from the powders prepared by mechanical alloying and mixing process.



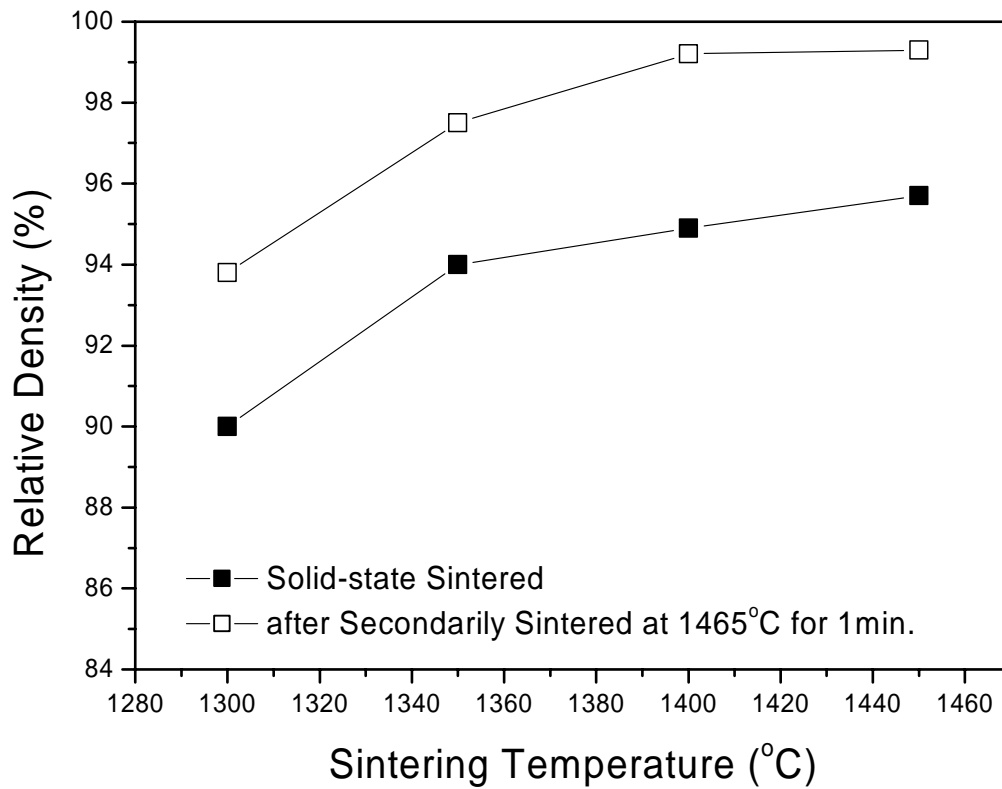


Fig. 10. Relative density of the secondarily sintered 94W-4.56Ni-1.14Fe-0.3Y<sub>2</sub>O<sub>3</sub> tungsten heavy alloys at 1465°C for 1 min after solid state sintering at temperature ranging from 1300 to 1450 °C for 1 hr from the powders prepared by mechanical alloying and mixing process..

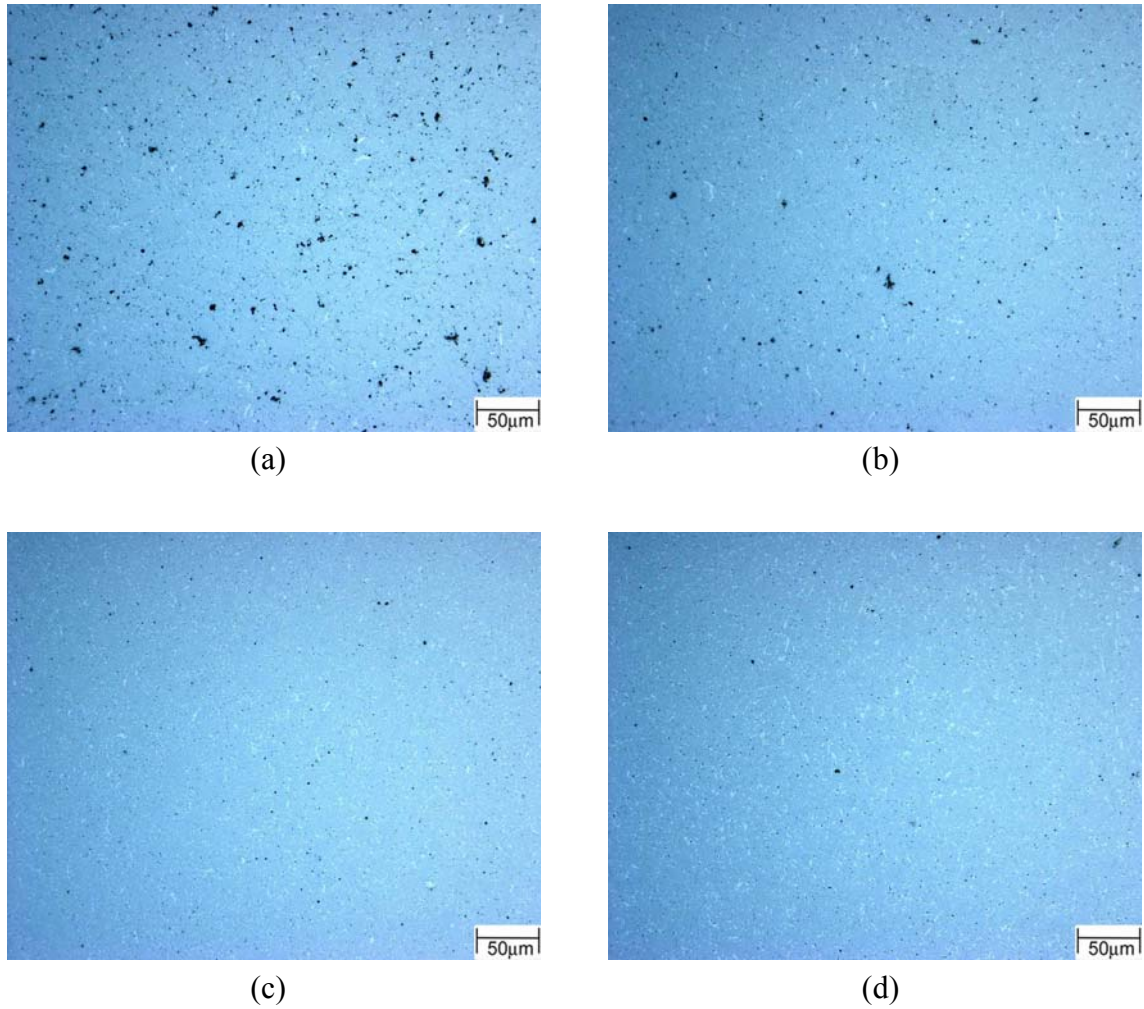
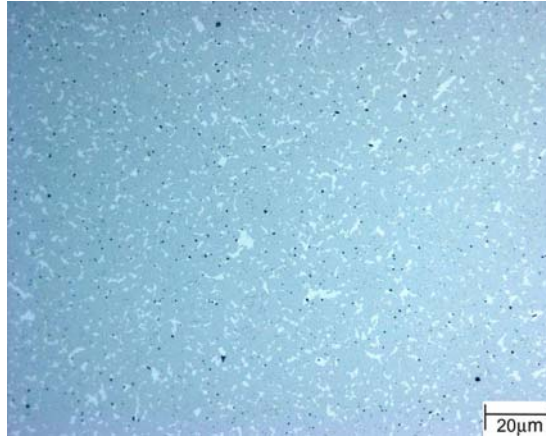
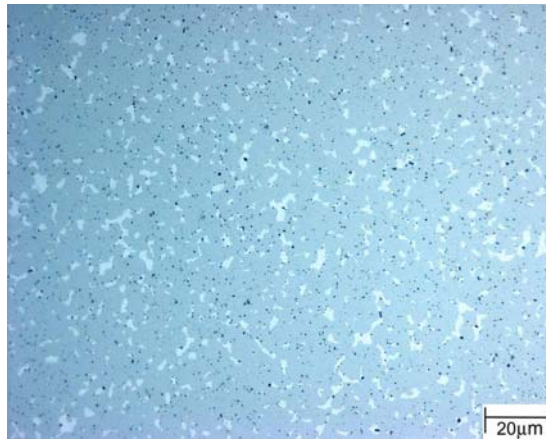


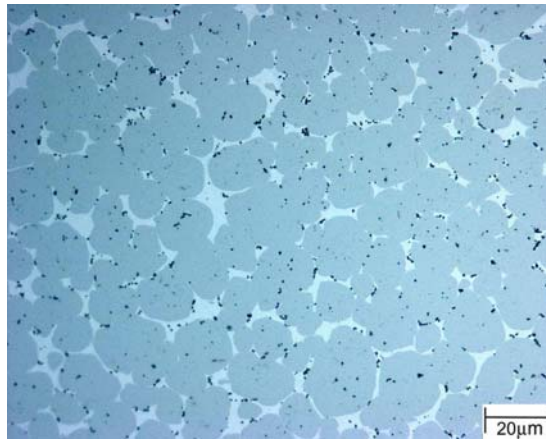
Fig. 11. Microstructure of the solid state sintered  $94\text{W}-4.56\text{Ni}-1.14\text{Fe}-0.3\text{Y}_2\text{O}_3$  tungsten heavy alloy at (a)  $1300^\circ\text{C}$ , (b)  $1350^\circ\text{C}$ , (c)  $1400^\circ\text{C}$  and (d)  $1450^\circ\text{C}$  for 1 hr from the powders prepared by two-step mechanical alloying process.



(a)

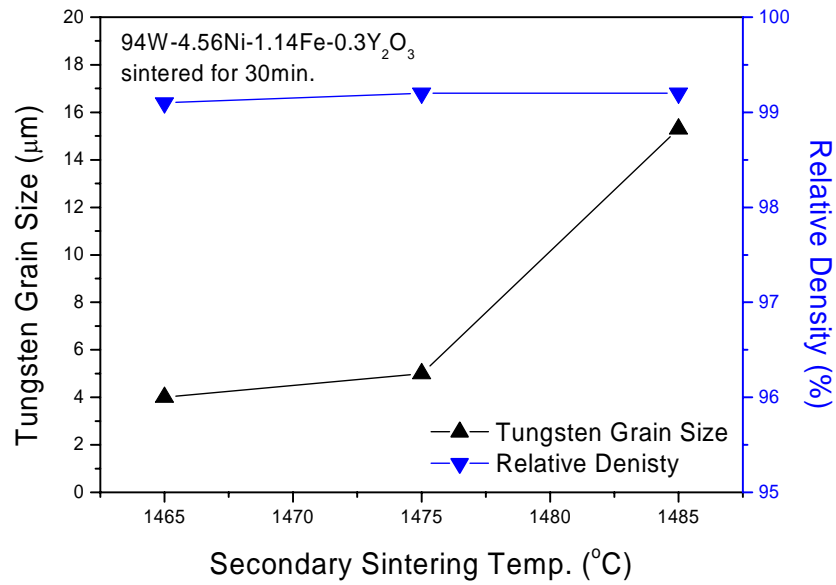


(b)

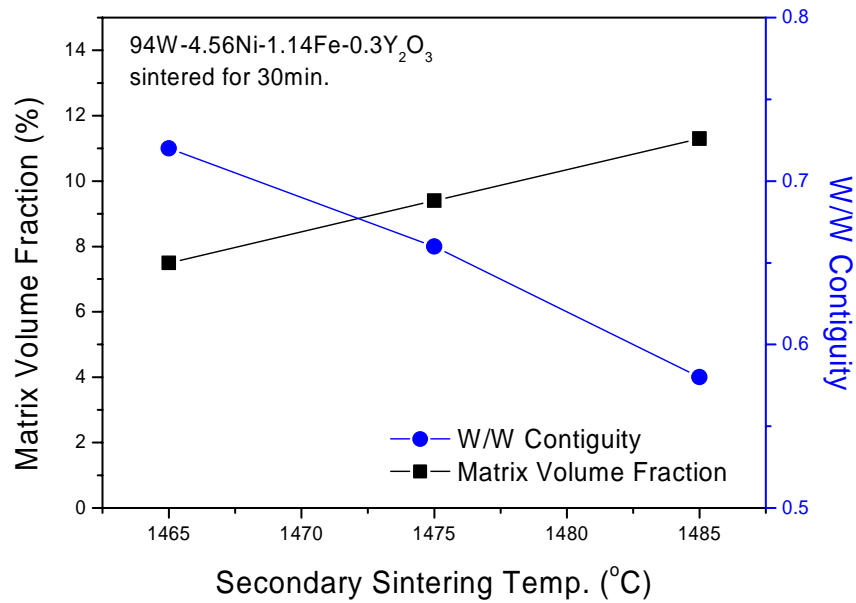


(c)

Fig. 12. Microstructure of two-stage sintered 94W-4.56Ni-1.14Fe-0.3Y<sub>2</sub>O<sub>3</sub> tungsten heavy alloys liquid phase sintered at (a) 1465 °C, (b) 1475 °C and (c) 1485 °C for 30 min after solid-state sintering at 1400 °C for 1 h.

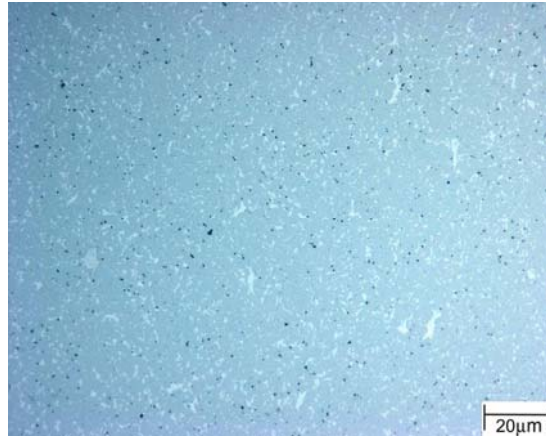


(a)

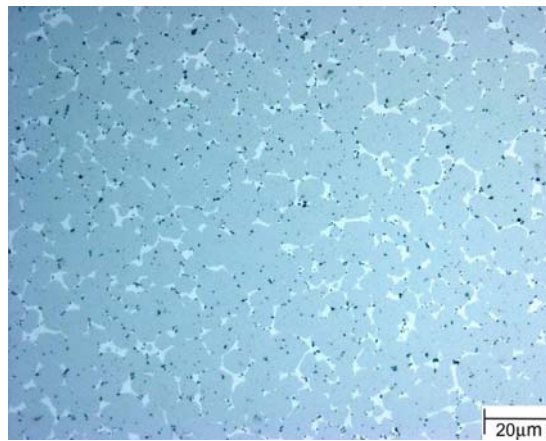


(b)

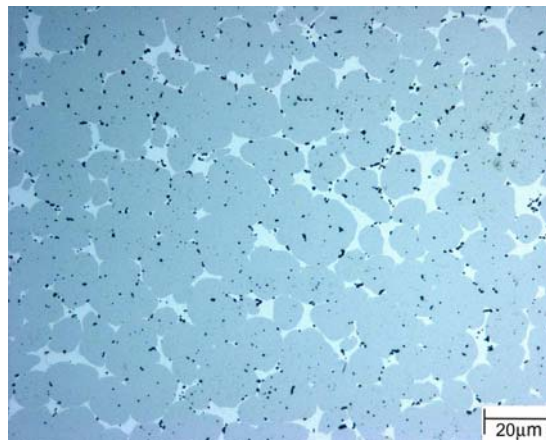
Fig. 13. The variation of (a) average tungsten grain size and relative density, and (b) matrix volume fraction and tungsten/tungsten contiguity of two-stage sintered 94W-4.56Ni-1.14Fe-0.3Y<sub>2</sub>O<sub>3</sub> alloys according to the secondary sintering temperature with fixed sintering time of 30 min.



(a)

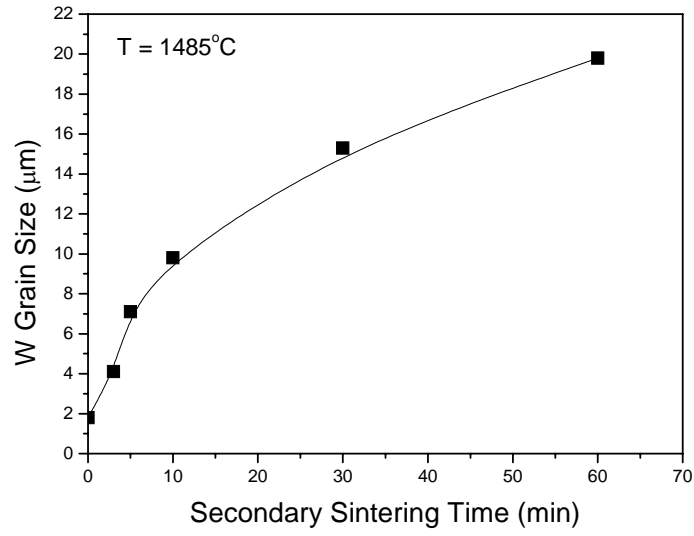


(b)

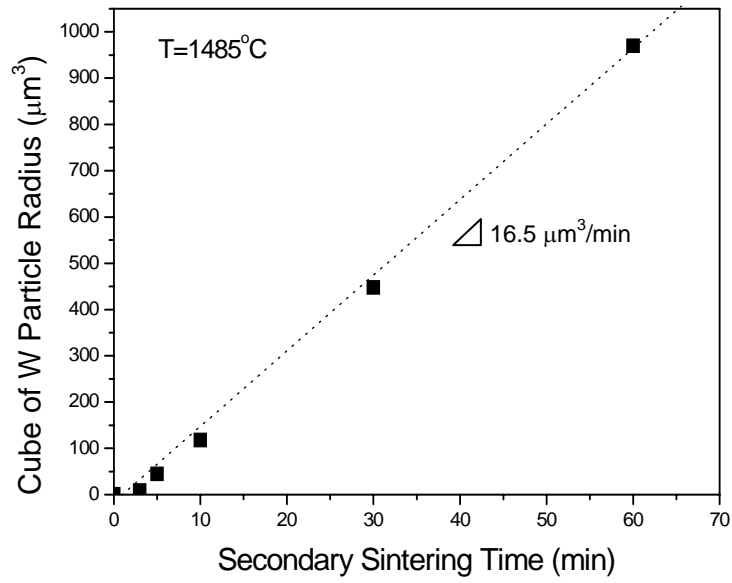


(c)

Fig. 14. Microstructure of two-stage sintered  $94\text{W}-4.56\text{Ni}-1.14\text{Fe}-0.3\text{Y}_2\text{O}_3$  tungsten heavy alloys secondarily sintered at  $1485\text{ }^\circ\text{C}$  for (a) 0 min, (b) 10 min and (c) 60 min after solid-state sintering at  $1400\text{ }^\circ\text{C}$  for 1 h.

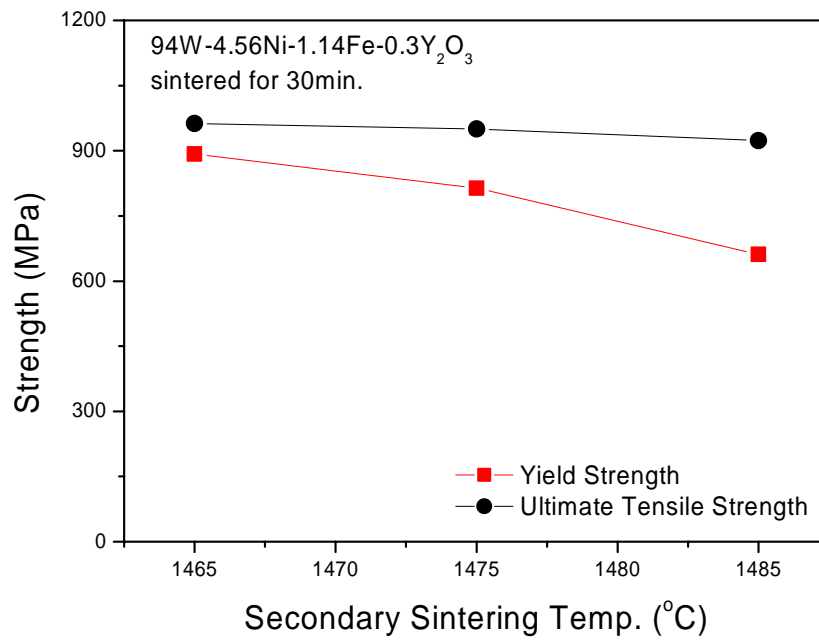


(a)

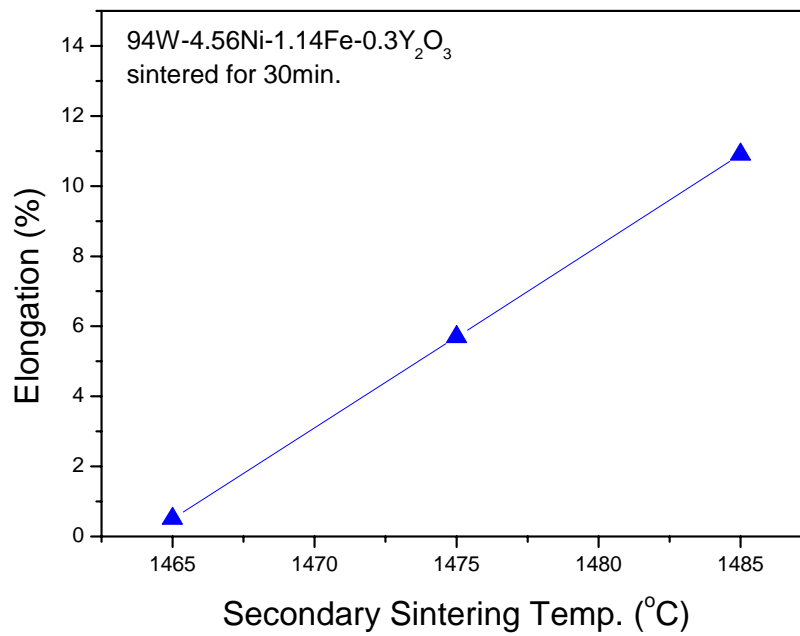


(b)

Fig. 15. (a) The variation of the tungsten grain size and (b) the variation of cubed tungsten grain radius with secondary sintering time of 94W-4.56Ni-1.14Fe-0.3Y<sub>2</sub>O<sub>3</sub> alloys, when the secondary sintering temperature was 1485°C.

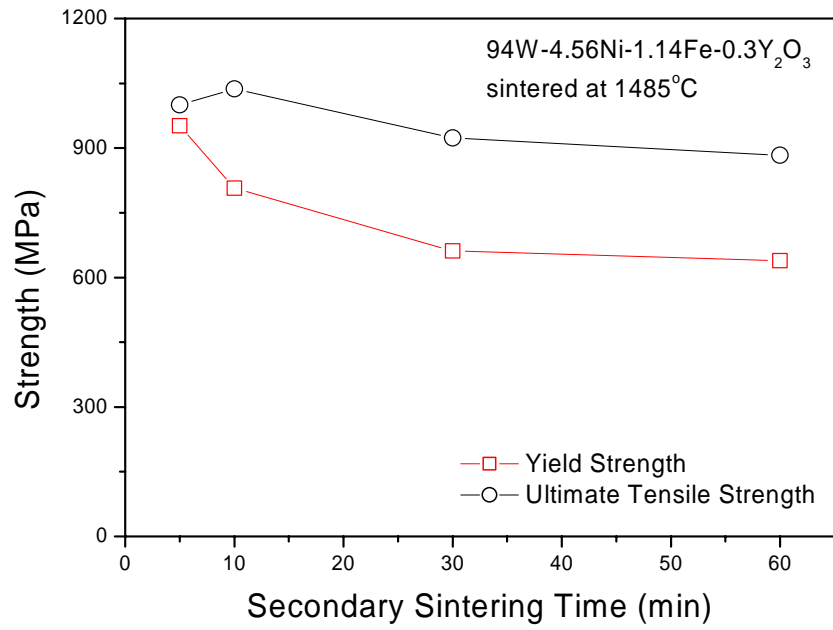


(a)

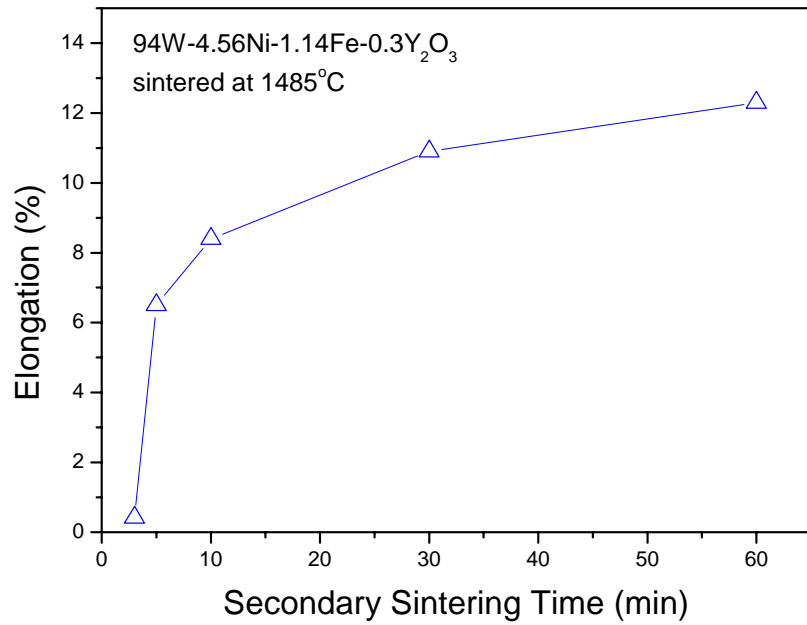


(b)

Fig. 16. Tensile strength and elongation of two-stage sintered 94W-4.56Ni-1.14Fe-0.3Y<sub>2</sub>O<sub>3</sub> tungsten heavy alloys with varying the secondary sintering temperature.



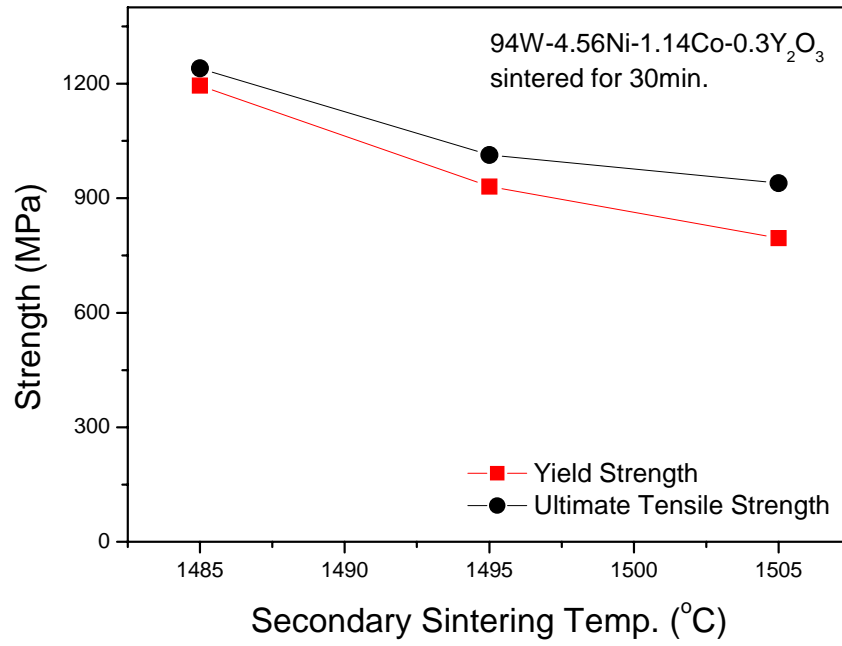
(a)



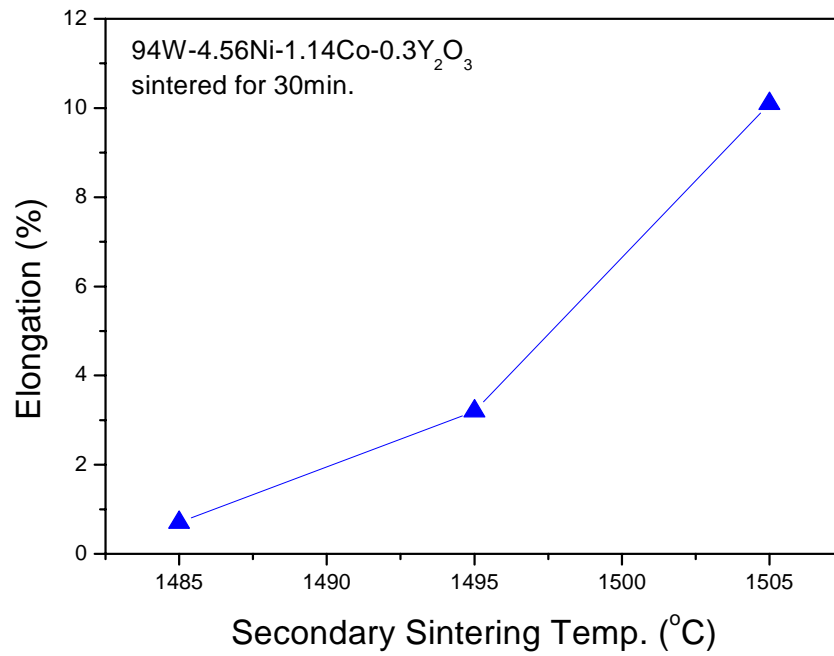
(b)

Fig. 17. Tensile strength and elongation of two-stage sintered 94W-4.56Ni-1.14Fe-0.3Y<sub>2</sub>O<sub>3</sub> tungsten heavy alloys with varying the secondary sintering time.



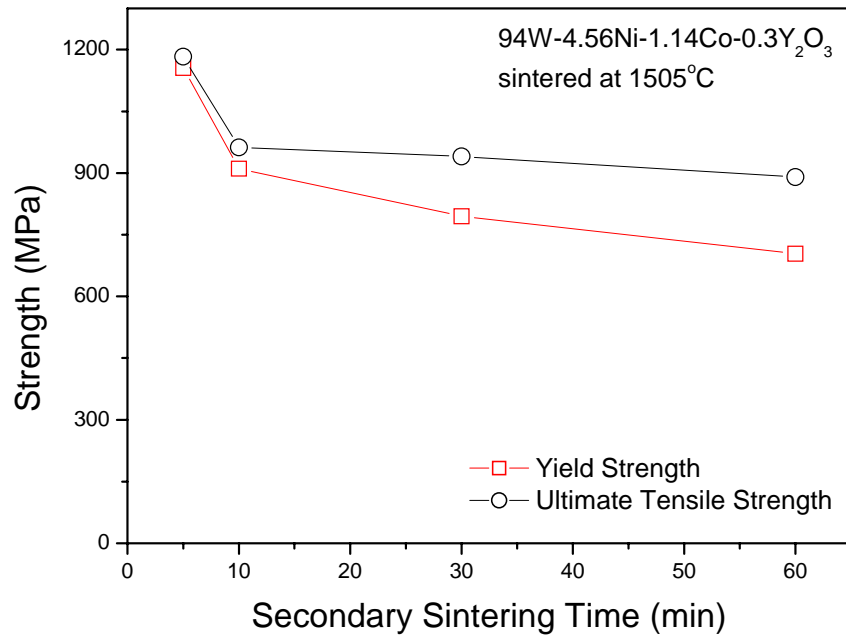


(a)

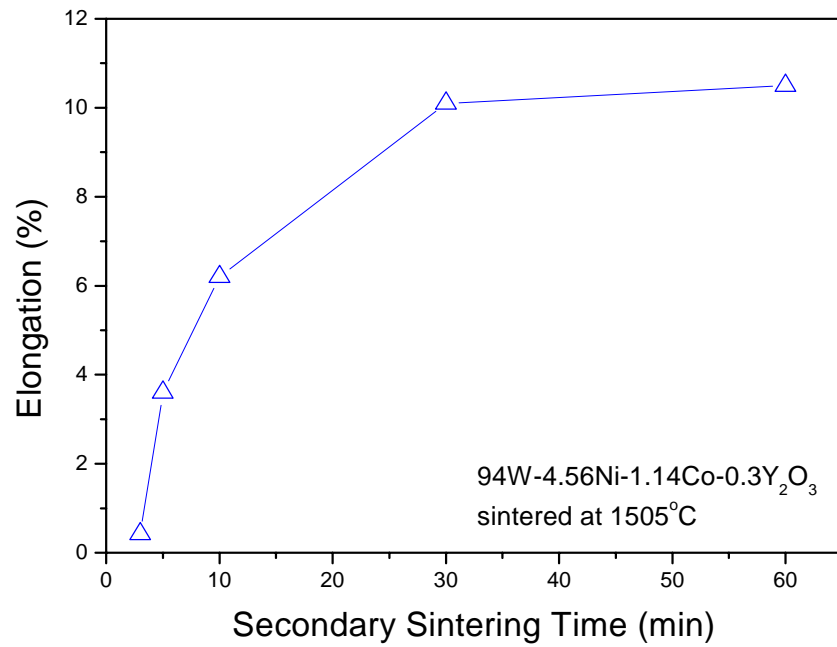


(b)

Fig. 18. Tensile strength and elongation of two-stage sintered 94W-4.56Ni-1.14Co-0.3Y<sub>2</sub>O<sub>3</sub> tungsten heavy alloys with varying the secondary sintering temperature.



(a)



(b)

Fig. 19. Tensile strength and elongation of two-stage sintered 94W-4.56Ni-1.14Co-0.3Y<sub>2</sub>O<sub>3</sub> tungsten heavy alloys with varying the secondary sintering time.

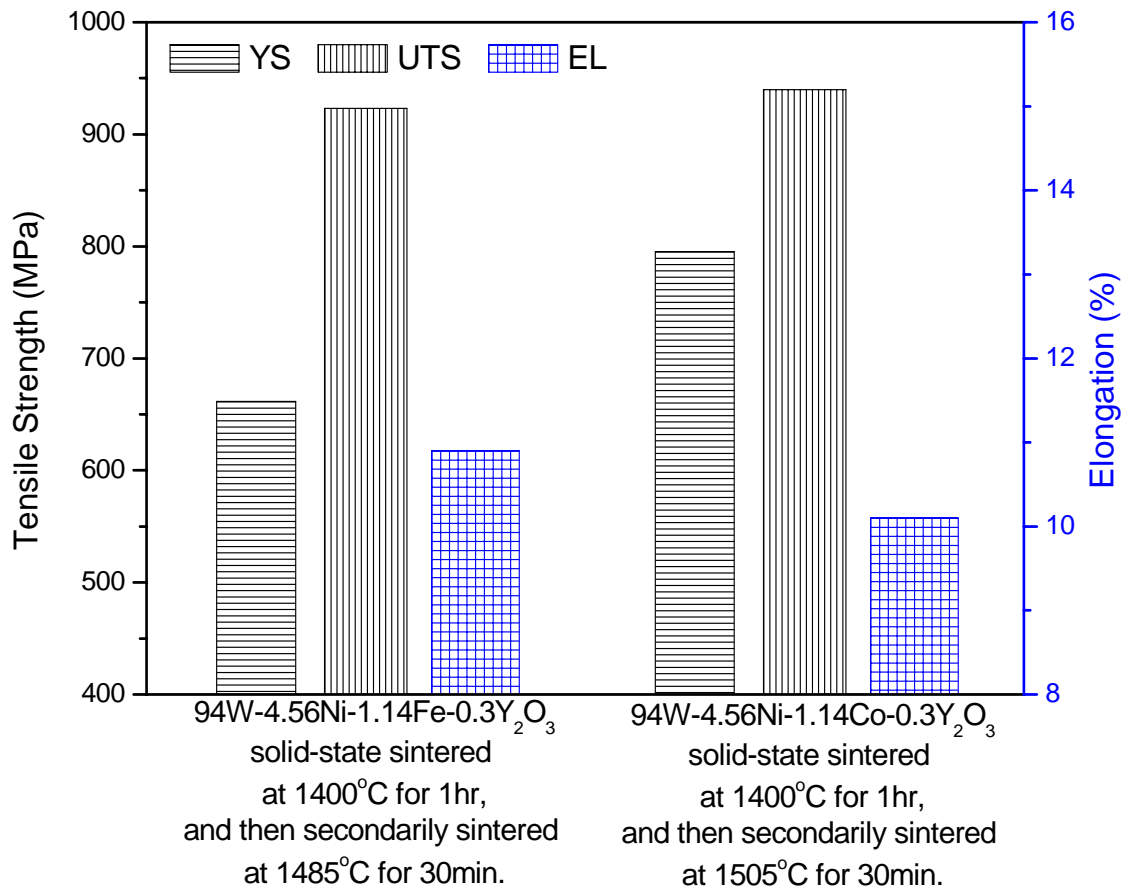


Fig. 20. Tensile properties of two-stage sintered ODS tungsten heavy alloys according to the composition.

### **3-3. Effect of cyclic heat-treatment process on microstructure and mechanical properties of ODS tungsten heavy alloys**

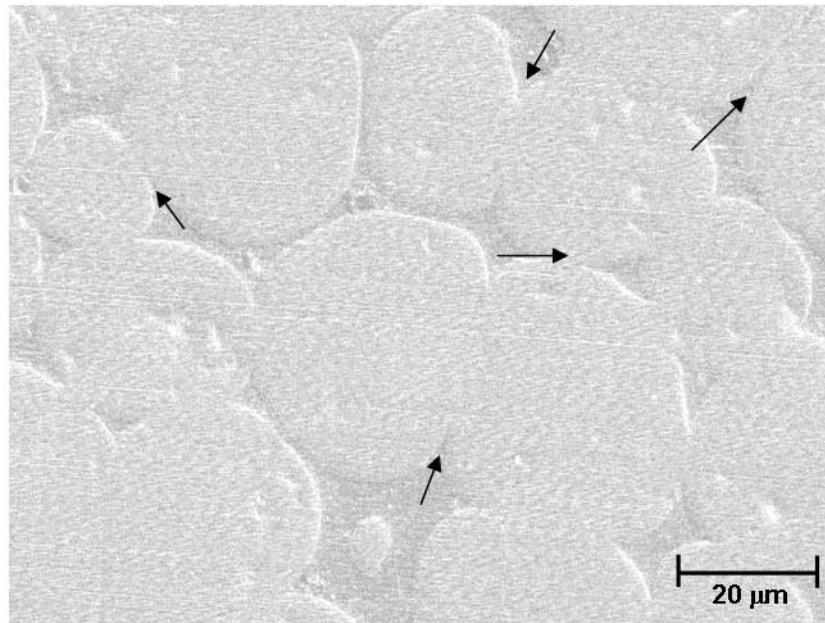
When the sintered ODS tungsten heavy alloys were cyclically heat-treated at 1150°C, the matrix phase is penetrated into tungsten/tungsten grain boundaries as shown in Fig. 21. The penetration of matrix phase was intensified with increasing the number of heat-treatment cycles. The tungsten/tungsten contiguity decreased from 0.56 to 0.41 with increasing the number of heat-treatment cycles from 1 to 10. The decrease of tungsten/tungsten grain boundary area in tungsten heavy alloys has been observed by performing cyclic heat-treatment with usual heat-treatment temperature and water quenching between the cycles [10, 11]. The tungsten/tungsten grain boundary area decreased with increasing the number of heat-treatment cycles for a fixed heat-treatment time. The matrix penetration by cyclic heat-treatment is due to the generation of thermal stress, which is induced during quenching from high temperature by the mismatch of thermal expansion coefficients between tungsten grain and matrix [10].

Yield strength and ultimate tensile strength of 94W-4.56Ni-1.14Co-0.3Y<sub>2</sub>O<sub>3</sub> alloy were maintained by the cyclic heat-treatment process as shown in Fig. 22. However, elongation of 94W-4.56Ni-1.14Co-0.3Y<sub>2</sub>O<sub>3</sub> alloy increased with increasing the number of heat-treatment cycles. The main effect of the cyclic heat-treatment is the drastic increase in impact energy due to the penetration of matrix between tungsten/tungsten grain boundaries in ODS tungsten heavy alloys [10]. Fig. 23 shows the improvement in the impact energy of ODS tungsten heavy alloys by cyclic heat-treatment.

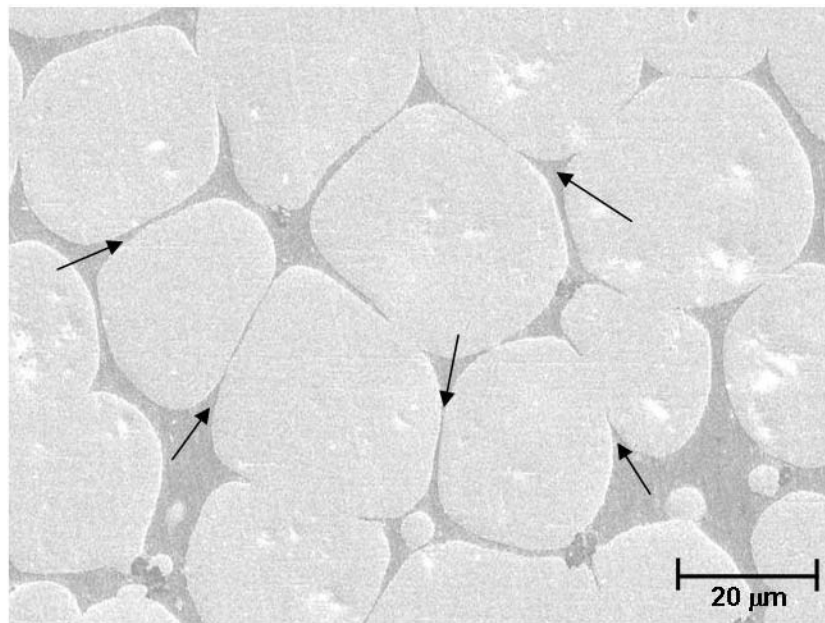
The above experimental results strongly suggest the improvement of mechanical properties by matrix penetration into tungsten/tungsten interface during the cyclic heat-treatment. It is well documented that thermal stress arises from the mismatch of thermal expansion coefficient between reinforcement and matrix during cooling in metal matrix composites. As the thermal expansion coefficients of Ni-Fe-W matrix and W grain are  $20 \times 10^{-6}$  K [10] and  $4.6 \times 10^{-6}$  K [12], respectively, tensile stress is induced in the matrix phase and compressive stress is applied in tungsten grains during rapid cooling from high temperature. The penetration of matrix into tungsten/tungsten grain boundaries, which was also observed in previous investigations [10], can be ascribed to the thermal stress developed during a cyclic heat-treatment. In the previous investigations [13], the generation of high thermal stress is confirmed by the observation of high dislocation density in the matrix phase

with increasing the number of heat-treatment cycles.

It is suggested that the mechanical properties, such as impact energy and elongation, can be controlled by controlling the tungsten/tungsten contiguity through cyclic heat-treatment of sintered ODS tungsten heavy alloys.



(a)



(b)

Fig. 21. Microstructure of 94W-4.56Ni-1.14Co-0.3Y<sub>2</sub>O<sub>3</sub> alloys sintered at 1505°C for 1hr, and then heat-treated at 1150°C for (a) 5 cycles and (b) 10 cycles. Arrows in the figures indicate matrix penetration into tungsten/tungsten interfaces.

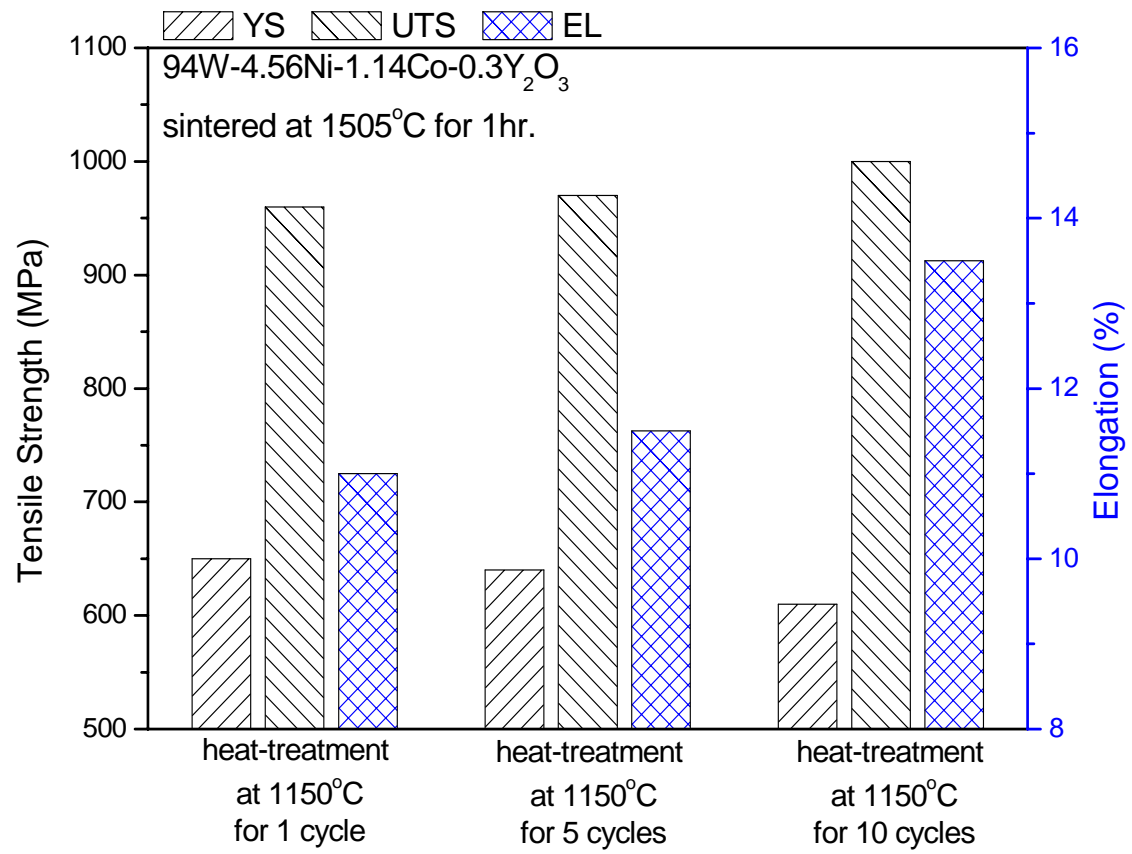


Fig. 22. Tensile properties of 94W-4.56Ni-1.14Co-0.3Y<sub>2</sub>O<sub>3</sub> alloys according to number of cycles for heat-treatment process.

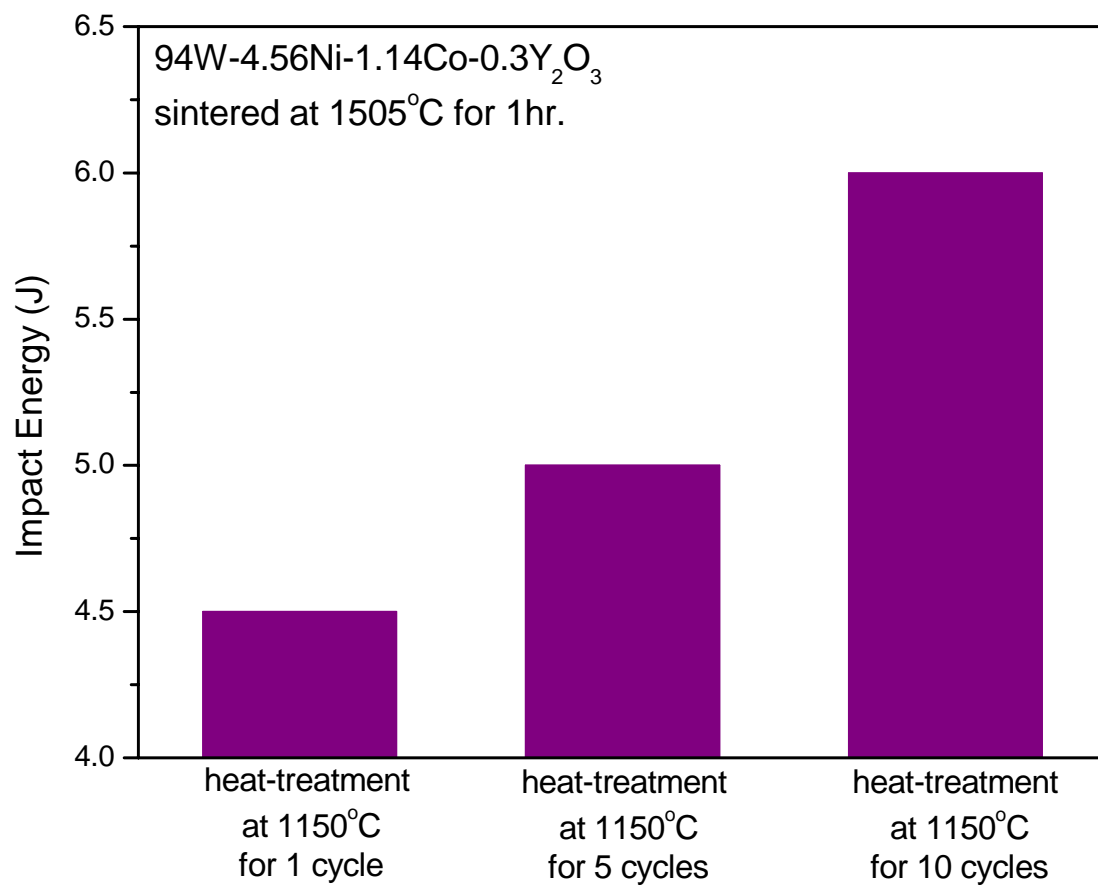


Fig. 23. The impact energy of 94W-4.56Ni-1.14Co-0.3Y<sub>2</sub>O<sub>3</sub> alloys according to number of cycles for heat-treatment process.



### 3-4. Relationship between microstructure and mechanical properties of ODS tungsten heavy alloys

Yield strength of tungsten heavy alloys can be formulated using the Hall-Petch type relationship as follows [8, 9],

$$\sigma_y = \sigma_0 + k_1 G b \rho^{1/2} \quad (2)$$

where  $\sigma_y$  is yield strength,  $\sigma_0$  is intrinsic strength,  $k_1$  is a constant,  $G$  is shear modulus,  $b$  is Burgers vector and  $\rho$  is dislocation density in matrix phase. As dislocation density,  $\rho$ , is inversely related to matrix thickness,  $\lambda$ , the yield strength can be expressed as,

$$\sigma_y = \sigma_0 + k_2 G b \lambda^{-1/2} \quad (3)$$

where  $k_2$  is a constant. Matrix thickness can be formulated in terms of tungsten grain size, tungsten/tungsten contiguity, and matrix volume fraction using geometrical relationship as follows,

$$\lambda = D \frac{V_M}{C_W(1 - V_M)} \quad (4)$$

where  $D$  is mean size of tungsten grains,  $C_W$  is tungsten/tungsten contiguity, and  $V_M$  is matrix volume fraction. The relationship between yield strength and microstructural parameters, i.e. tungsten grain size, tungsten/tungsten contiguity and matrix volume fraction, is expressed as following Eq.(5),

$$\sigma_y = \sigma_0 + k_2 G b \left( \frac{C_W(1 - V_M)}{D V_M} \right)^{1/2} \quad (5)$$

According to Eq.(5), yield strength of ODS tungsten heavy alloys increased with decreasing the tungsten grain size and matrix volume fraction. Fig. 24 shows that the yield strength of sintered ODS tungsten heavy alloys, which have a wide range of average tungsten grain size and matrix volume fraction, agreed well with Eq.(5). Therefore, it is concluded that the main deformation and yielding of ODS tungsten heavy alloys is caused by deformation of matrix at room temperature.

The addition of Mo below 2wt.% changes the intrinsic strength,  $\sigma_0$ , and the slope of line predicted by Eq. (5) maintaining a liner relationship between yield strengths and the microstructural factor following Eq. (5). Also, W-Ni-Co-Y<sub>2</sub>O<sub>3</sub> alloys showed same relationship with Eq. (5), but with different  $\sigma_0$  and slope as shown in Fig. 25.

The analysis of relationship, based on the Hall-Petch type relationship in Fig. 25, is suggested as a new method to compare the strengthening mechanism of ODS tungsten heavy alloys having different microstructural factors. In this method, the yield strength of various types of ODS tungsten heavy alloys can be compared with each other by normalizing the different microstructural factors. The new analysis is suggested as an advanced technique to analyze the intrinsic strengthening effects of alloying elements under different microstructural conditions.

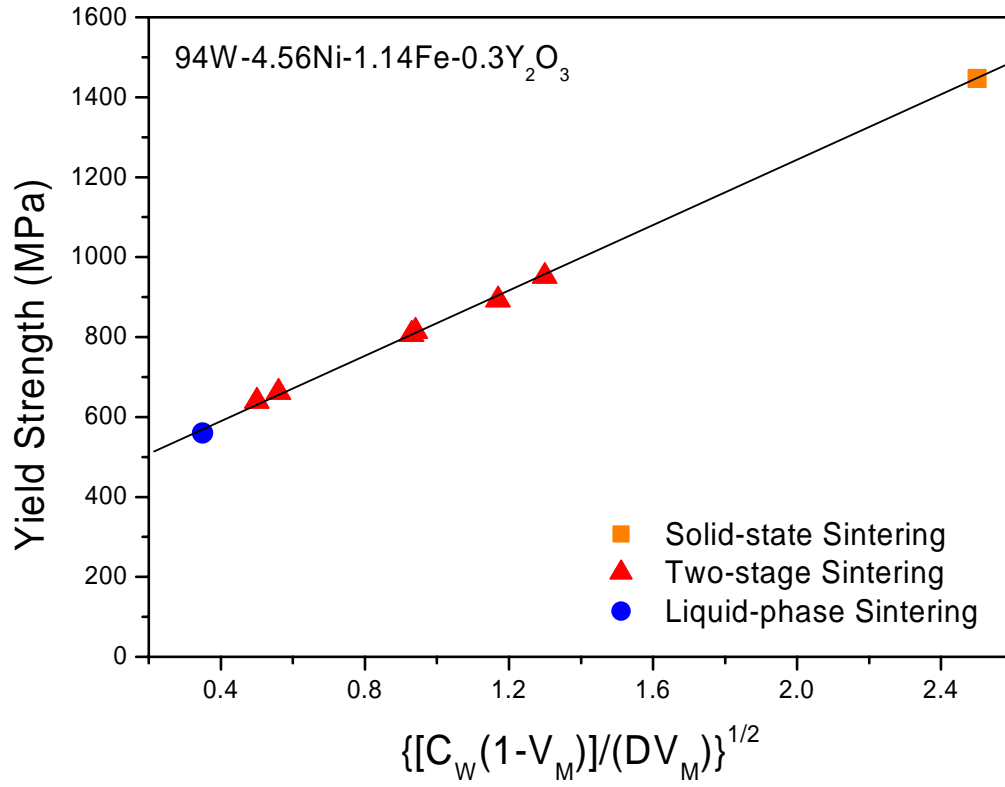


Fig. 24. Variation of yield strength as a function of microstructural parameters consisting of the matrix volume fraction,  $V_M$ , tungsten/tungsten contiguity  $C_W$  and tungsten grain size,  $D$ , of solid-state sintered, two-stage sintered, and liquid phase sintered 94W-4.56Ni-1.14Fe-0.3Y<sub>2</sub>O<sub>3</sub> alloys.

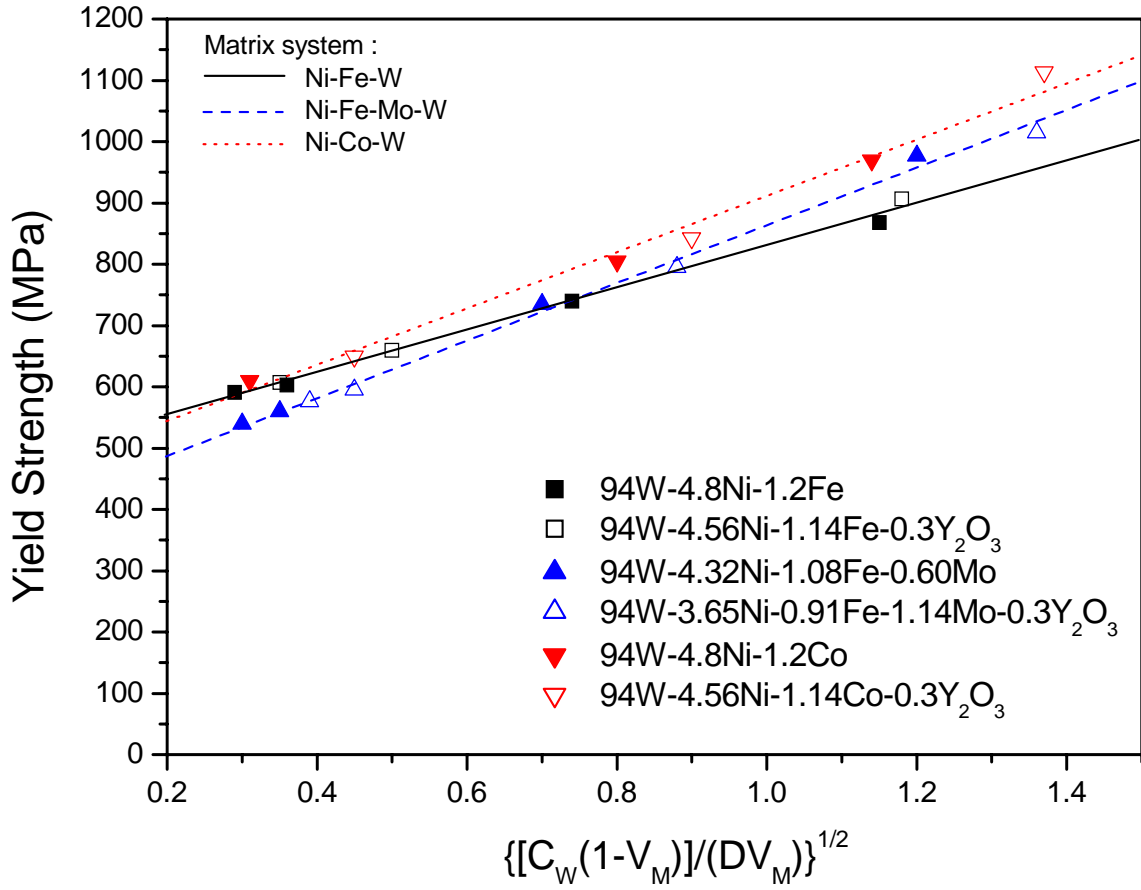


Fig. 25. Variation of yield strength as a function of microstructural parameters consisting of the matrix volume fraction,  $V_M$ , tungsten/tungsten contiguity  $C_W$  and tungsten grain size,  $D$ , of ODS tungsten heavy alloys according to the matrix modification.

#### 4. Summary

The microstructure and mechanical properties of ODS tungsten heavy alloys were investigated. The ODS tungsten heavy alloys were fabricated by mechanical alloying process followed by two-stage sintering process and cyclic heat-treatment process. The major results are summarized as follows;

- 1) Three new alloy systems were designed as 94W-4.56Ni-1.14Fe-0.3Y<sub>2</sub>O<sub>3</sub>, 94W-3.65Ni-0.91Fe-1.14Mo-0.3Y<sub>2</sub>O<sub>3</sub> and 94W-4.56Ni-1.14Co-0.3Y<sub>2</sub>O<sub>3</sub> alloys. Among three alloy systems, 94W-4.56Ni-1.14Co-0.3Y<sub>2</sub>O<sub>3</sub> alloy showed higher strength at room and elevated temperature, while showed lower elongation and impact energy than those of other alloys.
- 2) Comparing to the conventional liquid phase sintered ODS tungsten heavy alloys, tungsten grain size and matrix volume fraction were decreased and tungsten/tungsten contiguity of ODS tungsten heavy alloys was increased by solid state sintering. ODS tungsten heavy alloys showed ultra-fine tungsten grain size of 2μm with relative density above 97% when solid state sintered at 1400°C for 1hr. Solid state sintered ODS tungsten heavy alloy exhibited high tensile strength of 1450MPa due to the fine tungsten grain size and high tungsten content while it showed low elongation below 1% due to the low matrix volume fraction and the large tungsten/tungsten contiguity. Microstructure and mechanical properties of the two-stage sintered ODS tungsten heavy alloy were controlled by controlling the secondary sintering conditions. Two-stage sintered ODS tungsten heavy alloys showed finer tungsten grain size and higher tensile strength compared to the conventional liquid phase sintered ODS tungsten heavy alloys.
- 3) Cyclic heat-treatment process was suggested to control the tungsten/tungsten grain boundary area and mechanical properties. The penetration of matrix phase into the tungsten/tungsten grain boundaries was resulted from the controlled cyclic heat-treatment process. The cyclic heat-treatment resulted in a decrease in tungsten/tungsten contiguity and increases in elongation and impact energy by decreasing the tungsten/tungsten grain boundary area.
- 4) The yield strength of ODS tungsten heavy alloys was found to be dependent on the microstructural parameters consisting of tungsten grain size, matrix volume fraction and tungsten/tungsten contiguity, which can be controlled by the two-stage sintering process. Also, the strengthening effect according to the compositions can be analyzed with this relationship. The yield strength and ultimate tensile strength of ODS tungsten heavy alloys can be improved by two-

stage sintering process due to finer microstructure. The elongation and impact energy of ODS tungsten heavy alloys can be improved by cyclic heat-treatment process due to lower tungsten/tungsten contiguity.

## 5. References

- [1] H. J. Ryu and S. H. Hong, *Mat. Sci. and Eng. A*, **363**(1-2), (2003) 179.
- [2] Final Report for Contract Research (AOARD 034032)
- [3] A. Bose, G. Jerman, R.M. German, *Powder Met. Inter.* **21** (1989) 9.
- [4] J.H. Huang, G.A. Zhou, C.Q. Zhu, S.Q. Zhang and H.Y. Lai, *Materials Letters* **23** (1995) 47.
- [5] R.M. German, L.L. Bourguignon and B.H. Rabin *J. Met.* **37** (1985), p. 36.
- [6] I.M. Lifshitz and V.V. Slyozov *J. Phys. Chem. Solids* **19** (1961), p. 35.
- [7] C. Wagner *Z. Electrochem.* **65** (1961), p. 581.
- [8] M.F. Ashby, *Phil. Mag.* **18** (1970) 399.
- [9] H. J. Ryu and S. H. Hong and W.H. Baek, *Mat. Sci. and Eng. A* **291**, (2000) 91.
- [10] J.W. Noh, E.P. Kim, H.S. Song, W.H. Baek, K.S. Churn and S-J.L. Kang, *Metall. Trans. A*, **24A** (1993) 2411.
- [11] H.S. Song, J.W. Noh, W.H. Baek and S.W. Lee, *J. Mat. Proc. Tech.*, 63 (1997) 618.
- [12] C.J. Smithells : Metal Reference Book, 4<sup>th</sup> ed., Butterworth and Co., London, vol.3 (1967) 687.
- [13] J.W. Noh, M.H. Hong, G.H. Kim, S.-J.L. Kang and D.N. Yoon, *Metall. Trans. A*, **25** (1994) 2828.